



Consensus Entropy: Harnessing Multi-VLM Agreement for Self-Verifying and Self-Improving OCR

Yulong Zhang^{1,2,3*}, Tianyi Liang^{4,3*}, Xinyue Huang⁵, Erfei Cui^{2,3}, Xu Guo³, Pei Chu³, Chenhui Li⁴,
Ru Zhang¹, Wenhai Wang³, Gongshen Liu^{2†}

¹Beijing University of Posts and Telecommunications, China ²Shanghai Jiao Tong University

³Shanghai Artificial Intelligence Laboratory ⁴East China Normal University ⁵Sun Yat-sen University

*These authors contributed equally †Corresponding author
yulong.z@bupt.edu.cn, lgshen@sjtu.edu.cn

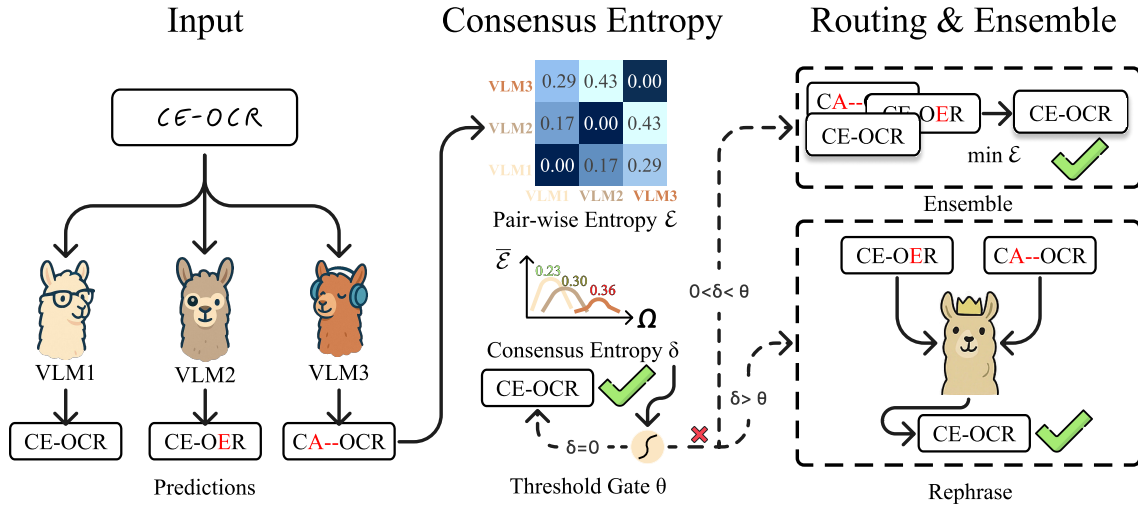


Figure 1: Overview of the CE-OCR framework. Given an input image, three Vision-Language Models (VLMs) independently generate OCR predictions. The pairwise similarities among predictions are used to compute a probability distribution over consensus quality, from which the *Consensus Entropy* δ is derived. Based on δ , a threshold gate θ determines the next step: if entropy is low, a consensus-based ensemble prediction is accepted; if entropy exceeds a predefined threshold, the system routes the input to a stronger VLM for rephrasing. This framework enables automatic self-verification and quality improvement of OCR outputs without training or supervision.

ABSTRACT

The Optical Character Recognition (OCR) task is important for evaluating Vision-Language Models (VLMs) and providing high-quality data sources for LLM training data. While state-of-the-art VLMs show improved average OCR accuracy, they still struggle with sample-level quality degradation and lack reliable automatic detection of low-quality outputs. We introduce Consensus Entropy (CE), a training-free post-inference method that quantifies OCR uncertainty by aggregating outputs from multiple VLMs. Our approach exploits a key insight: correct VLM OCR predictions converge in output space while errors diverge. We develop a lightweight multi-model framework that effectively identifies problematic samples, selects the best outputs and combines model strengths. Experiments across multiple OCR benchmarks and VLMs demonstrate that CE outperforms VLM-as-judge approaches and single-model baselines at the same cost and achieves state-of-the-art results across multiple metrics. For instance, our solution demonstrates: achieving 15.2%

higher F1 scores than VLM-as-judge methods in quality verification, delivering 6.0% accuracy gains on mathematical calculation tasks, and requiring rephrasing only 7.3% of inputs while maintaining overall performance. Notably, the entire process requires neither training nor supervision while maintaining plug-and-play functionality throughout.

CCS CONCEPTS

• **Computing methodologies** → **Information extraction**; Machine learning; • **Applied computing** → **Document analysis**.

KEYWORDS

Optical Character Recognition, Vision-Language Model, Training-Free

1 INTRODUCTION

The Optical Character Recognition (OCR) task serves as a critical bridge connecting textual information in the physical world

with digital information systems. Therefore, the quality and diversity of OCR-derived data crucially determine the reliability and generalization capability of large language models (LLMs), as it constitutes one of the most important pipelines for acquiring real-world textual data to fuel AI training processes [21, 45, 54]. In recent years, the rapid progress of Vision-Language Models (VLMs) [3, 10–12, 17, 18, 35, 56] has transformed OCR capabilities from task-specific algorithms into a core component of multimodal perceptual understanding. Consequently, OCR accuracy has become a critical metric for assessing the visual-linguistic reasoning capacity of such models. At the same time, the scarcity of high-quality OCR data and the high cost of manual annotation have made both the evaluation of data quality and the assessment of model outputs enduring challenges in OCR research.

Current OCR evaluation frameworks predominantly rely on standardized benchmark metrics [15, 37, 61], creating a disconnect between reported performance and real-world reliability. Our extensive document understanding experiments with state-of-the-art models, including Qwen2.5-VL-72B [3] and GPT4o [42], reveal that even top-performing VLMs exhibit **frequent semantic inaccuracies and formatting inconsistencies that evade detection by conventional metrics**. Notably, models with higher benchmark scores sometimes underperform in practical applications compared to those with slightly lower benchmark rankings. Current evaluation approaches fall into two categories with distinct limitations: multimodal re-evaluation based on cross-validation is constrained by the evaluation models’ own uncertainties and often introduces secondary noise [6, 19, 28, 64, 65], while VLM-as-judge methods for textual quality assessment cannot effectively verify the consistency between visual inputs and textual outputs. **The lack of OCR-specific uncertainty quantification approach for visual-textual alignment** significantly hampers the development of trustworthy OCR systems for real-world applications.

We conduct a systematic analysis of OCR predictions produced by a variety of VLMs, and identify three underlying characteristics of OCR output behavior: (1) OCR tasks generally exhibit a unique semantic ground truth which can be directly compared, despite variations in formatting; (2) in regions where models perform well, predictions tend to converge with high consistency, forming dense consensus clusters; (3) incorrect predictions typically display pronounced semantic divergence and high entropy. Based on these observations, we propose a novel uncertainty quantification approach—**Consensus Entropy (CE)**—to capture the degree of agreement among multiple model predictions for the same input image. Our CE framework computes pairwise similarities between VLM outputs and measures the entropy of their distribution as an uncertainty indicator. We propose CE-Guided routing: low-entropy predictions are deemed reliable and merged, while high-entropy cases are redirected to specialized models. We conduct empirical evaluations of CE across multiple OCR benchmarks and VLM. The results demonstrate its effectiveness in a variety of practical scenarios, including quality filtering, ensemble prediction, and uncertainty-aware training. **Our contributions are three-fold:**

- We introduce **Consensus Entropy (CE)**, a novel uncertainty metric for OCR, quantifying prediction reliability based on inter-model agreement.

- We propose a training-free CE-guided ensemble strategy with adaptive routing, enabling automatic quality-aware OCR that selectively combines multiple models’ strengths or redirects to stronger models for challenging cases.
- We validate CE across diverse OCR tasks and VLMs, demonstrating its effectiveness in output evaluation, data selection, and performance enhancement at the same output tokens.

2 RELATED WORK

Evaluating OCR Capabilities of Multimodal Large Models.

Optical character recognition has evolved from early commercial tools [1] to modern approaches divided into pipeline systems [2, 48, 55] and end-to-end models [5, 58]. Recent multimodal large models have demonstrated impressive OCR capabilities, evaluated through both module-level benchmarks (OCR-Bench [15, 37], CC-OCR [61] and PubLayNet [60]) and page-level assessments accompanying VLM-driven expert models [5, 34, 58]. However, these benchmarks suffer from limitations in data diversity and evaluation scope. System-level approaches like olmOCR [45] and MinerU [22, 55] enhance document understanding, but a critical limitation persists: existing frameworks focus primarily on global accuracy metrics, obscuring individual output reliability—particularly problematic when OCR results serve as inputs for downstream models. While CC-OCR [61] represents progress in comprehensive evaluation, the challenge of assessing individual output quality remains largely unaddressed. Our proposed Consensus Entropy method directly addresses this gap by providing a **training-free approach** to quantify output reliability at the instance level.

Limitations of LLM-Based Evaluation. Current evaluation approaches for OCR outputs rely heavily on the "LLM-as-Judge" paradigm [28, 64, 65], where language models serve as automated evaluators. However, comprehensive surveys [6, 19] identify systematic weaknesses in this approach, including sensitivity to prompt wording [38], training data contamination [51], and format biases [32]. A particularly concerning issue is preference leakage [30], where correlations between generation and evaluation models produce artificially inflated judgments. These limitations become more pronounced in adversarial settings [4, 46], leading to inconsistent assessments. Traditional metrics like BLEU [43] and ROUGE [33] similarly fail to capture semantic accuracy in OCR tasks. Moreover, LLM evaluators struggle with multimodal understanding tasks that require precise document layout comprehension [23], which are essential for OCR involving complex layouts and mathematical content. Our Consensus Entropy framework **overcomes these limitations by providing model-agnostic quality** assessment without reliance on potentially biased evaluators.

Uncertainty Estimation and Multi-Model Agreement. Recent advances in uncertainty quantification span three complementary paradigms: probabilistic methods modeling parameter uncertainty [16, 27, 36], token-level confidence estimation for hallucination detection [8, 24, 41], and latent space techniques capturing fine-grained variations [44, 57]. For cross-modal tasks, recent work explores semantic entropy analysis [63] and calibrated confidence metrics [7, 59], while multi-model consensus approaches leverage disagreement as a reliability signal [13, 25].

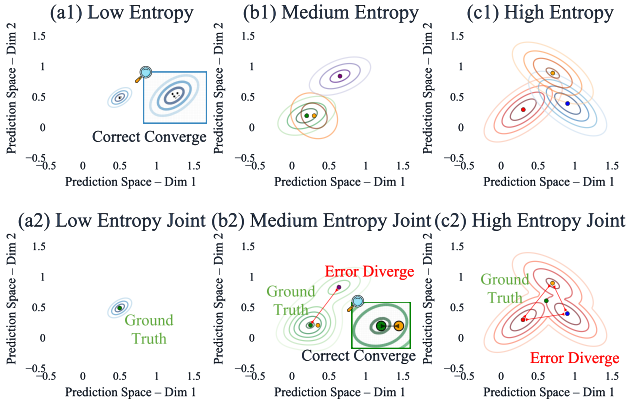


Figure 2: Prediction behaviors across entropy levels. Each plot visualizes VLM predictions in a 2D space. In low-entropy cases (a), predictions tightly cluster around the ground truth (green), while in medium (b) and high-entropy (c) settings, predictions increasingly diverge.

LLM ensemble strategies have evolved along two primary paths: selection-based approaches that identify optimal outputs from candidate pools [20, 31, 50] and selection-then-regeneration techniques that synthesize improved outputs from high-quality candidates [9, 26, 40, 53]. However, current uncertainty quantification research predominantly addresses general LLM text generation [57, 59], largely overlooking OCR-specific challenges. Existing approaches fail to leverage a critical OCR characteristic: *correct predictions consistently converge semantically despite formatting variations*, creating an opportunity for lightweight, calibration-free uncertainty quantification tailored specifically to visual text recognition tasks.

3 METHOD

Our framework, as illustrated in Figure 1, addresses the fundamental challenge of uncertainty quantification in OCR tasks through a novel multi-model agreement approach. At its core lies the Consensus Entropy metric, **which transforms the problem of quality assessment from a supervised evaluation task into an unsupervised agreement analysis.**

3.1 Consensus Entropy

We introduce Consensus Entropy (CE), a novel approach to OCR quality assessment that requires no ground truth supervision. Our method builds on a key insight illustrated in Figure 2: when multiple independent models process the same image, **correct outputs naturally converge in semantic space while error outputs diverge.** This pattern of convergence and divergence serves as a powerful signal for estimating output quality without requiring labeled data.

Our framework begins by collecting outputs from a set of independent OCR models $\mathcal{M} = \{M_1, M_2, \dots, M_n\}$ for an image I . Each output is represented as an embedding vector in a shared semantic space using a pre-trained text encoder. To quantify the prediction

agreement across models, we first calculate the pairwise entropy \mathcal{E} between all model output pairs:

$$\mathcal{E}_{ij} = - \sum_k p_{ij}(k) \log p_{ij}(k), \tag{1}$$

where $p_{ij}(k)$ is the probability distribution derived from the semantic similarity between the i -th and j -th model outputs at position k . Unlike cosine similarity which provides only a single scalar value, our entropy-based approach captures the distributional uncertainty in the alignment between outputs.

For each model output, we then compute its average entropy distance to all other outputs:

$$\bar{\mathcal{E}}_i = \frac{1}{n-1} \sum_{j \neq i} \mathcal{E}_{ij}. \tag{2}$$

This average entropy distance $\bar{\mathcal{E}}_i$ quantifies how consistent each model’s output is with the collective predictions—lower values indicate outputs that align well with the consensus.

To model the overall distribution of these outputs in the semantic space, we employ **kernel density estimation (KDE)** with adaptive bandwidth, which allows us to capture the underlying probability density of the prediction manifold:

$$p(\mathbf{v}) = \sum_{i=1}^n w_i \cdot \mathcal{N}(\mathbf{v}|\mathbf{v}_i, \Sigma_i), \tag{3}$$

where w_i is inversely proportional to $\bar{\mathcal{E}}_i$, giving greater weight to outputs with lower entropy distance (higher consensus), and $\mathcal{N}(\mathbf{v}|\mathbf{v}_i, \Sigma_i)$ is a multivariate Gaussian kernel centered at \mathbf{v}_i with covariance matrix Σ_i that adapts based on the local density of predictions.

In practice, we discretize the semantic space using an $N \times N$ grid. The final Consensus Entropy δ is computed as:

$$\delta = - \sum_{i=1}^{N^2} p_i \log p_i, \tag{4}$$

where p_i is the probability at cell i in the grid. This discretization enables efficient computation while maintaining accuracy.

To identify the optimal strategy for combining probability distributions in our CE framework, we evaluated four aggregation methods: Sum, Max, Mean, and Mean Distance. As shown in Figure 3, we examined how these methods perform across different grid resolutions and entropy levels. Importantly, all methods maintain consistent preference ordering across conditions, indicating the robustness of our entropy-based approach. The Mean Distance method, which directly averages the $\bar{\mathcal{E}}$ values, demonstrates particularly effective discrimination in high-entropy scenarios while maintaining computational efficiency. The Sum method similarly shows consistent behavior across distribution types. Based on these comparative results, we selected **the Mean Distance method** as our primary implementation, with Sum serving as a viable alternative for scenarios requiring different sensitivity profiles. Additional detailed analyses of the CE framework are provided in the appendix.

As shown in Figure 2, this entropy value effectively captures **the degree of agreement among model predictions.** In low-entropy scenarios (Figure 2a), predictions form tight clusters around

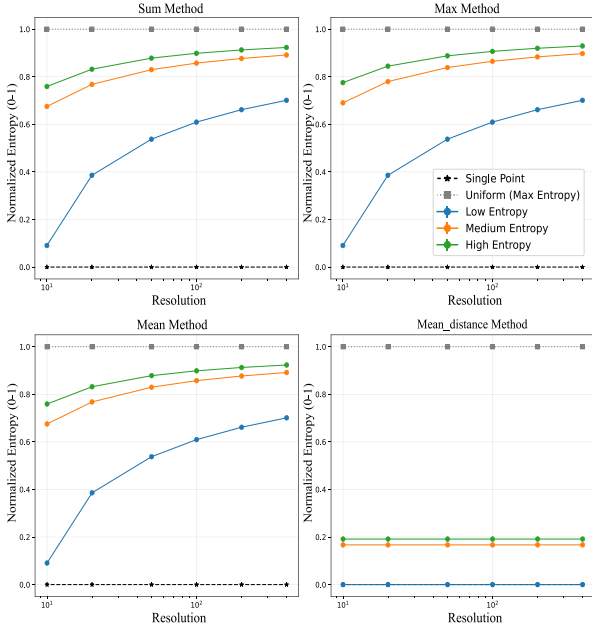


Figure 3: Normalized entropy (0-1) analysis of four combination methods across different distribution types and grid resolutions. Single point distribution (dashed line) and uniform distribution (dotted line) serve as lower and upper bounds. Error bars represent standard deviation over five runs.

the ground truth, indicating high confidence. In contrast, medium-entropy (Figure 2b) and high-entropy (Figure 2c) settings show progressively greater divergence, signaling increasing uncertainty about the correct transcription.

The Consensus Entropy δ serves as our core uncertainty metric—lower values indicate higher agreement and likely correctness, while higher values signal potential errors or ambiguities. This metric provides a direct measure of output reliability **without requiring ground truth labels, enabling fully unsupervised quality assessment at scale**. As referenced in Figure 1, δ serves as the key decision signal in our routing framework, determining whether to accept ensemble predictions or seek expert refinement.

3.2 Ensemble and Router

The CE framework is designed to be flexible and adaptable, allowing for various ensemble strategies and routing mechanisms based on the computed Consensus Entropy. The core idea is to **leverage the entropy value to guide the decision-making process** for handling OCR outputs, balancing between efficiency and quality.

3.3 Threshold Gate and Routing Mechanism

After computing Consensus Entropy δ , we introduce a **threshold-based routing mechanism to balance efficiency and quality**. The key component is a threshold gate parameter θ that determines how outputs are processed:

Algorithm 1 Consensus Entropy for Multi-Model OCR Evaluation

Require: $\{O_1, O_2, \dots, O_n\}$ - n OCR models outputs for image I
Require: σ - base kernel bandwidth parameter
Require: α - adaptive bandwidth scaling factor
Require: N - grid resolution for probability density estimation

```

// Compute pairwise entropies and weights
for  $i = 1$  to  $n$  do
    for  $j = 1$  to  $n, j \neq i$  do
         $\mathcal{E}_{ij} \leftarrow \text{ComputePairwiseEntropy}(O_i, O_j)$ 
    end for
     $\bar{\mathcal{E}}_i \leftarrow \frac{1}{n-1} \sum_{j \neq i} \mathcal{E}_{ij}$  {Average entropy distance}
     $w_i \leftarrow \frac{1/\bar{\mathcal{E}}_i}{\sum_{k=1}^n 1/\bar{\mathcal{E}}_k}$  {Normalize weights}
     $\Sigma_i \leftarrow \sigma \cdot (1 + \alpha \cdot \bar{\mathcal{E}}_i) \cdot \mathbf{I}$  {Adaptive covariance}
end for
// Project outputs to semantic space and estimate distribution on  $N \times N$  grid
 $\{\mathbf{v}_1, \mathbf{v}_2, \dots, \mathbf{v}_n\} \leftarrow \text{ProjectToSemanticSpace}(\{O_1, O_2, \dots, O_n\})$ 
 $P \leftarrow \text{EstimateDistributionOnGrid}(\{\mathbf{v}_i, w_i, \Sigma_i\}_{i=1}^n, N)$ 
// Calculate entropy from  $N \times N$  grid-based distribution
 $\delta \leftarrow -\sum_{x=1}^N \sum_{y=1}^N P[x, y] \cdot \log P[x, y]$  {Discrete entropy calculation on  $N \times N$  grid}
return  $\delta$  {Return Consensus Entropy}
    
```

$$R(\delta, \theta) = \begin{cases} 0, & \text{if } \delta \leq \theta \\ 1, & \text{if } \delta > \theta, \end{cases} \quad (5)$$

where $R(\delta, \theta) = 0$ indicates using the ensemble output, and $R(\delta, \theta) = 1$ triggers routing to a stronger VLM.

This parameter θ serves as a critical decision boundary that can be adjusted based on task-specific requirements, as illustrated in Figure 1. Lower thresholds prioritize quality by routing more samples to expert models, while higher thresholds favor computational efficiency by accepting more ensemble predictions.

We calibrate θ through empirical analysis on development data, identifying the entropy value that optimizes the quality-efficiency trade-off. Our experiments **indicate that θ values between 0.3 and 0.5** provide the best balance for most OCR tasks, effectively identifying high-quality predictions while routing only the most problematic samples for expert processing.

3.4 Ensemble Strategy

When Consensus Entropy falls below the threshold ($\delta \leq \theta$), we apply a weighted ensemble strategy to combine predictions from multiple models. Unlike simple averaging approaches, our weights directly leverage the entropy framework:

$$O_{\text{ens}} = \sum_{i=1}^n w_i \cdot O_i, \quad (6)$$

where the weighting coefficients w_i are derived from the average entropy distances $\bar{\mathcal{E}}_i$:

$$w_i = \frac{1/\bar{\mathcal{E}}_i}{\sum_{j=1}^n 1/\bar{\mathcal{E}}_j}. \quad (7)$$

Human Score Band	GPT4o		Qwen2-VL-7B		Qwen2-VL-72B	
	VLM-J	CE	VLM-J	CE	VLM-J	CE
0.9-1.0	0.7212	0.5729	0.7005	0.7088	0.7227	0.6613
0.7-0.8	0.1842	0.4019	0.1982	0.3956	0.2301	0.4014
0.4-0.6	0.2147	0.3867	0.0000	0.2734	0.1143	0.2847
0.0-0.3	0.4821	0.6544	0.5474	0.6742	0.5283	0.6957
Overall	0.40	0.48 (↑0.08)	0.36	0.51 (↑0.15)	0.40	0.51 (↑0.11)

Table 1: Comparison of F1 scores between human annotations, VLM-as-Judge (VLM-J) models, and our CE method. The VLM-as-Judge approach employs different VLM models to score the predictions of Qwen2.5-VL-72B by prompting them with task-specific instructions. In contrast, the Consensus Entropy (CE) method uses different models to generate predictions on the same OCR inputs and computes a CE score between each model’s output and the prediction from Qwen2.5-VL-72B.

This approach assigns **higher weights to outputs with lower entropy distances** (higher consensus), while **downweighting outputs with higher entropy distances** (potential outliers).

In practice, implementing this weighted combination for text requires a token-level aggregation approach. We first align all outputs using **dynamic programming to identify corresponding tokens across predictions**. Then, for each position, we select the token with the highest weighted consensus, computed as:

$$t_k^* = \operatorname{argmax}_{t \in T_k} \sum_{i: t \in O_i} w_i, \quad (8)$$

where T_k is the set of all candidate tokens at position k across model outputs, and the sum aggregates weights from all models whose outputs contain token t at that position.

3.5 Expert Routing

When Consensus Entropy exceeds the threshold ($\delta > \theta$), indicating low agreement among models, we route the sample to a more powerful VLM (referred to as M_{exp}) for rephrasing. This stronger model processes the input image along with the ensemble prediction and original model outputs as context:

$$O_{\text{final}} = M_{\text{exp}}(I, \{O_1, O_2, \dots, O_n\}, O_{\text{ens}}). \quad (9)$$

This approach allows the stronger VLMs to benefit from the collective wisdom of the ensemble while having the capacity to correct errors and resolve ambiguities. Importantly, this model is prompted to focus specifically on areas of disagreement, making efficient use of its computational resources. The complete algorithm incorporating threshold gating, ensemble strategy, and selective routing to a stronger model is presented in Algorithm 3 in the Appendix.

This framework enables a dynamic, quality-aware OCR pipeline that automatically adapts to input complexity. By leveraging Consensus Entropy to guide both ensemble aggregation and expert routing decisions, **we achieve superior OCR performance without requiring additional training or supervision.**

4 EXPERIMENTS

This section is structured to thoroughly evaluate our Consensus Entropy framework. We assess CE’s ability to evaluate OCR quality

without supervision, select optimal outputs from multiple models, and improve performance through a flexible framework.

4.1 Experimental Setup

Implementation Details. Our experimental evaluation is based on the inference outputs from a wide range of models. Most models align with the default settings provided by *vllm* [14], except for simulations on real-world datasets which rely on outputs from vLLM Inference Framework [29]. It is important to note that our experiments **solely involve model inference without any training, significantly reducing computational overhead**. For inference, all models except the largest ones, such as Qwen2.5-VL-72B and other models above 70 billion parameters, use a single NVIDIA H800 (80GB) GPU. The aforementioned larger models require between 2 to 4 NVIDIA H800 (80GB) GPUs for inference. The entire set of inference experiments was completed in less than one week, demonstrating the efficiency of our experimental setup.

Datasets for Evaluation. Our research utilizes three datasets: OCRBench [37], OCRBench-V2 [15], and CCOCR [61], with the majority of our experiments conducted on OCRBench [37]. Additional experiments and detailed analyses are presented in the appendix. To align our evaluation with human preferences in real-world contexts, we also curated a unique dataset consisting of 1,000 PDF pages randomly selected from actual scenarios. These documents were processed using the state-of-the-art Qwen2.5-VL-72B [3] model to perform OCR tasks. The resultant texts were manually compared to the original PDF pages, and each was assigned a quality score ranging from 1.0 (Perfect Match) to 0.0 (Mostly Incorrect), with varying degrees of text matching accuracy. This diverse dataset collection allows for a comprehensive assessment of OCR performance across various domains, languages, and formatting complexities, providing insights into both machine efficiency and human-centric accuracy. Detailed scoring criteria and methodology are available in Appendix Table 9.

4.2 Baselines

We establish two representative baseline approaches. These methods are widely adopted in current applications of VLMs, and serve as comparative references across varying levels of complexity and supervision.

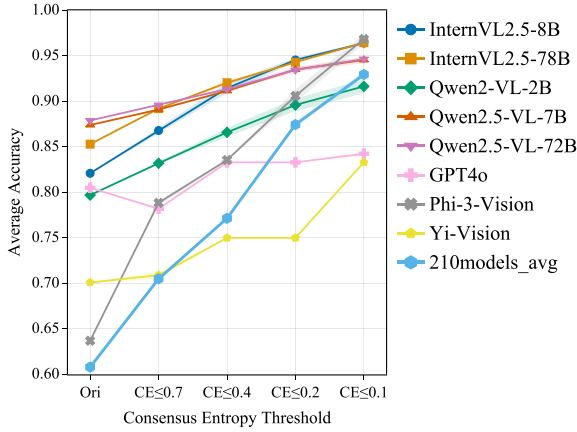


Figure 4: Model Performance on OCRBench under Different CE Thresholds. CE values are computed with two reference models (ref1: Qwen2-VL-7B, ref2: Qwen2-VL-72B[56]), The 210models_avg, representing the average performance of 210 models, demonstrates the wide applicability of CE in filtering correct outputs from VLMs. The shaded area is formed by the accuracy curves of ref1 and ref2, while the solid line represents their average.

VLM-as-Judge. This baseline follows the mainstream paradigm of using large language models as evaluators to score candidate outputs. Specifically, we employ GPT4o [42], Qwen2-VL-72B [56], and Qwen2-VL-7B [56] as evaluation models, each guided by standardized prompts to assess OCR output quality. The evaluation criteria emphasize semantic correctness, visual-text alignment, and structural fidelity.

Single Model Output. To better highlight the performance gains introduced by Consensus Entropy, we adopt a direct single-model output strategy as a baseline. In this setting, each image is processed by a single VLM (e.g., GPT4o [42] or Qwen2.5-VL-72B [3]), and its raw prediction is used as the final result without post-processing. This configuration reflects common practice in many real-world OCR applications and provides a conservative lower-bound reference for evaluating the effectiveness of our framework.

4.3 Unsupervised Self-Verifying with CE

Our goal is twofold: (1) to assess whether Consensus Entropy can effectively identify the most accurate OCR outputs without supervision, and (2) to determine whether it surpasses the VLM-as-Judge approach in real-world OCR tasks involving multi-document content, by better aligning with human accuracy and preferences.

Experimental Setups. We evaluate CE’s effectiveness in identifying correct OCR outputs across multiple VLMs. Our implementation uses three reference models: GPT4o [42], Qwen2-VL-72B, and Qwen2-VL-7B [56]. The evaluation is conducted on OCRBench, where we analyze the relationship between CE thresholds and model accuracy.

CE Threshold Analysis. Figure 4 illustrates the relationship between CE thresholds and model accuracy across different VLMs.

Table 2: Statistical Analysis of Performance Gains from CE-Guided Ensemble Outputs. This table summarizes average improvements (Δ_{\max} , Δ_{\min} , Δ_{avg}) and the proportion of negative cases across 3, 4, and 5 model ensembles using CE-based output selection.

Size	Mean Δ_{\max}	Mean Δ_{\min}	Mean Δ_{avg}	Δ_{\max}^- Ratio	Δ_{\min}^- Ratio	Δ_{avg}^- Ratio
3	50.2	4.2	28.3	0.3%	33.8%	5.3%
4	67.5	12.7	41.7	0%	17.8%	0.14%
5	78.3	17.8	50.3	0.3%	8.89%	0.01%

The results show a clear trend: as the CE threshold decreases, the average accuracy of model responses increases. **This pattern holds true for the majority of the 210 VLMs tested, including both open-source and proprietary models.**

Human Evaluation Comparison. Utilizing our curated dataset of 1,000 PDF pages from real-world scenarios, which includes documents of various languages, types, and complexities, we compared the CE method with the VLM-as-Judge approach. Results in Table 1 show that CE method consistently achieves higher F1 scores, ranging from 0.479 to 0.513, compared to 0.361 to 0.400 for the VLM-as-Judge. This marks an average improvement of 15.2% in accurately identifying high-quality OCR outputs. **The robustness of CE across various document complexities highlights its effectiveness for practical OCR applications.**

4.4 Multi-VLM Ensemble with CE

Experimental Setups. We conduct multi-model ensemble experiments using OCRBench, which comprises 1,000 manually curated question-answer pairs across five representative text understanding tasks. The ensemble policy is just to calculate CE with models and choose the We collect OCR outputs from 24 mainstream VLM models and evaluate all unique combinations of multiple models.

Enhanced Ensemble Performance Analysis. We evaluate ensembles of different sizes: 3-model ($C_{24}^3 = 2024$ combinations), 4-model ($C_{24}^4 = 10626$ combinations), and 5-model ($C_{24}^5 = 42504$ combinations). Table 2 present the performance of CE-driven ensembles on OCRBench. Key findings reveal that as more models are integrated into the ensemble, the overall effectiveness improves significantly, evidenced by increasing Δ_{\max} , Δ_{\min} , and Δ_{avg} values with larger ensemble sizes. Specifically, CE consistently selects outputs that outperform the weakest and even the strongest models in the ensemble across all model combinations, as indicated by consistently positive Δ_{\min} values and almost non-existent negative Δ_{\max} occurrences. Notably, the Δ_{\min}^- Ratio and Δ_{avg}^- Ratio demonstrate that even in scenarios where the ensemble performance might not surpass the best individual model, the CE ensemble’s outputs generally exceed the ensemble average and closely approach the performance of the best model. This trend is particularly pronounced in larger ensembles, where the Δ_{avg}^- Ratio approaches zero, highlighting CE’s robustness and its ability to leverage collective model strengths effectively.

High-Performance & Representative Ensemble Analysis. Table 3 presents the highest-scoring CE-driven ensembles, including both high-performing and notably interesting combinations. Several ensembles not only achieve scores beyond the current state-of-the-art (SOTA) score of 926, but also demonstrate the potential of CE to

Table 3: High-Scoring & Representative CE-Ensembles. We list high-scoring and representative CE-driven ensemble outputs from 3, 4, and 5-model combinations. Ensembles highlighted in blue comprise exclusively open-source VLMs with fewer than 10 billion parameters, demonstrating CE’s effectiveness in resource-constrained scenarios. Blue highlights indicate the best scores, while green highlights mark the best individual models and their scores.

Ensemble Size	Models in Ensemble	Individual Scores	Ensemble Score	Improv. over Best
5	Ovis2-1B [39], Qwen2.5-VL-72B [3], SenseChat-Vision [47], Step1V [52], Step1o [52]	890, 879, 894, 886, 926	958	+32
	Qwen2-VL-7B [56], Qwen2.5-VL-72B [3], Qwen2.5-VL-7B [3], Ovis2-8B [39], Ovis2-4B [39]	843, 879, 874, 893, 909	926	+17
	MiniCPM-V-2_6 [62], Ovis2-1B [39], Ovis2-4B [39], Ovis2-8B [39], Qwen2.5-VL-7B [3]	852, 890, 909 , 893, 874	930 (+21)	
4	Ovis2-1B [39], Qwen2.5-VL-7B [3], Step1V [52], Step1o [52]	890, 874, 886, 926	955	+29
	Qwen2-VL-7B [56], Qwen2.5-VL-72B [3], Ovis2-4B [39], MUG-U-7B [49]	843, 879, 909, 911	932	+21
	Ovis2-1B [39], Ovis2-4B [39], Qwen2-VL-7B [56], Qwen2.5-VL-7B [3]	890, 909 , 843, 874	933 (+24)	
3	Ovis2-8B [39], SenseChat-Vision [47], Step1o [52]	893, 894, 926	941	+15
	InternVL2.5-78B [10], Qwen2.5-VL-72B [3], Qwen2-VL-72B [56]	853, 879, 888	920	+32
	InternVL2.5-8B [10], Qwen2.5-VL-7B [3], Qwen2.5-VL-72B [3]	821, 874, 879	902	+23
	InternVL2.5-8B [10], Qwen2-VL-7B-Instruct [56], Qwen2.5-VL-7B [3]	821, 843, 874	897	+23

enhance the capabilities of large models (over 70B parameters) and commercial closed-source models with the assistance of smaller models. **The best five-model ensemble reaches a score of 958**, while high-performing four- and three-model ensembles achieve scores of 955 and 941, respectively. Noteworthy is the performance of ensembles composed exclusively of lightweight open-source VLMs with fewer than 10 billion parameters. These ensembles can surpass the 926 benchmark, demonstrating CE’s effectiveness in resource-constrained scenarios. For instance, **an ensemble of small open-source models (3B, 7B, 8B) surpasses the scores of commercial closed-source SOTA models like Step1o [52] and MUG-U-7B [49]**, as well as the open-source SOTA model Qwen2.5-VL-72B [3]. This highlights the potential of CE to leverage smaller models to challenge and even outperform larger, more resource-intensive models.

4.5 CE Framework for Self-Improving OCR

Experimental Setups. To evaluate the effectiveness of our CE Framework for Self-Improving OCR, we conducted comprehensive experiments across OCRBench-V2, covering various visual text understanding tasks. We set the CE threshold at 0.5 for routing decisions; inputs with CE values below this threshold are processed using weighted ensemble outputs, while those above are routed to a stronger VLM for rephrasing. Table 4 presents performance comparisons for specific OCR-related task categories from OCRBench-V2.

Results Analysis. Our CE Framework demonstrates superior performance over both individual models and basic ensemble approaches

Table 4: Performance comparison of CE Framework against individual models and basic ensemble across different OCR task categories in OCRBench-V2 [15].

Method	English Text Recognition	Mathematical Calculation	Chinese Element Parsing	Chinese Overall
GPT4o	0.612	0.434	0.298	0.322
InternVL2.5-26B	0.612	0.477	0.309	0.432
Gemini Pro	0.656	0.374	0.326	0.442
Ensemble	0.672	0.501	0.340	0.457
CE Framework (Rephrase)	0.716	0.531	0.338	0.460

across a broad spectrum of OCR tasks, particularly excelling in complex scenarios such as mathematical calculations, where **it achieves a 6.0% accuracy improvement over conventional ensembles**. The framework’s efficacy is derived from its dynamic selection mechanism based on CE values. Inputs with high consensus among models leverage weighted ensemble outputs, while those with low consensus are directed to a stronger VLM for improved prediction. This selective routing strategy optimizes resource utilization, with **only 7.3% of inputs necessitating stronger model rephrasing**. By quantifying uncertainty and effectively integrating the strengths of multiple models, the framework offers a practical, training-free solution for diverse real-world OCR challenges. As shown in Figure 5, the Self-Consistency (SC@3) models in our framework consistently outperform their single-model counterparts across different token lengths. The visualization demonstrates that models using our approach maintain higher cumulative scores as token length increases.

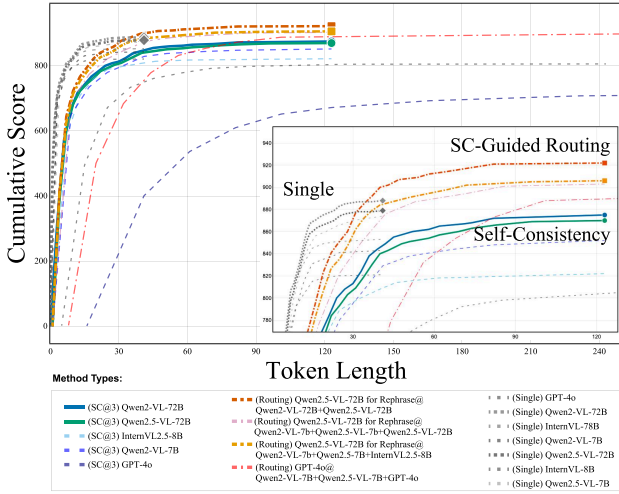


Figure 5: OCR Performance Comparison. Cumulative scores of different models plotted against token length, with Self-Consistency (SC@3) models in blue, Routing models in orange, and Single models in gray. Top performers in each category shown with thicker lines.

Table 5: Performance comparison of different OCR methods based on cumulative scores. SC@3 represents Self-Consistency with 3 samples, Routing refers to the ensemble with rephrasing, and Single indicates individual model performance.

Method	Score	Improvement (%)
SC@3 (Average)	828	-2.8
SC@3 (Best: Qwen2-VL-72B)	875	2.7
Routing (Average)	907	6.5
Routing (Best: Qwen2.5-VL-72B)	922	8.2
Single (Average)	852	-
Single (Best: Qwen2-VL-72B)	888	-

4.6 Ablation Study

Table 6 presents the results of our ablation study. As part of our comprehensive analysis, we evaluated three key components of the CE Framework: (1) the Consensus Entropy calculation, (2) the multi-model ensemble strategy, and (3) the adaptive routing mechanism.

Impact of Consensus Entropy Calculation. CE is pivotal to our framework, enabling precise uncertainty quantification. As indicated in Table 6, removing CE leads to a notable performance decline, underscoring its critical role in selecting the optimal outputs. Furthermore, **CE consistently outperforms traditional VLM-as-Judge methods in identifying high-quality OCR outputs, achieving F1 scores between 0.479 and 0.513 compared to 0.361 to 0.400 by VLM methods—an average improvement of 15.2%.** This improvement demonstrates CE’s capability in assessing OCR quality based on model output patterns, without explicit supervision.

Table 6: Ablation study results on OCRBench. We examine the CE Framework with different components removed. The score represents OCRBench evaluation metrics.

Configuration	Score \uparrow	% Routed	Rel. Perf.
w/o CE (Single Model Max)	0.888	0%	97.9%
w/o Ensemble (Single Model Avg)	0.852	0%	93.9%
w/o Routing (All Ensemble)	0.902	0%	99.4%
Full CE Framework	0.907	7.3%	100%

Effects of Multi-Model Ensemble. Our multi-model ensemble significantly enhances the framework’s performance. Data from Table 3 show that even the best individual models fall short against CE-guided ensembles. Ablation studies (Table 6) reveal that substituting the ensemble with **single models (average score 888.92) leads to a marked 7.2% performance drop.**

Contribution of Adaptive Routing. Adaptive routing optimizes resource allocation while maintaining high accuracy. As shown in Table 6, the model without routing (using ensemble for all inputs) **achieves 99.4% of the full framework’s performance**, demonstrating the robustness of the CE-guided ensemble approach. The key advantage of adaptive routing is its computational efficiency: the full framework requires stronger vlm rephrasing for only 7.3% of inputs while maintaining nearly identical performance to processing all inputs with the ensemble.

Our experiments show that the three components—CE, multi-model ensemble, and adaptive routing—work synergistically, enhancing the framework’s overall effectiveness. The diversity of the model ensemble enriches the data for CE, improving uncertainty quantification. Similarly, the success of the routing mechanism hinges on precise entropy estimation. The integrated approach demonstrates how our framework effectively addresses OCR reliability and efficiency without additional training or labeled data, while minimizing computational resources through highly selective routing to stronger models.

5 CONCLUSION

This work has introduced a fundamental shift in how OCR quality can be assessed without reliance on labeled data or expensive human evaluation. By leveraging the natural convergence of correct predictions and divergence of errors across multiple VLMs, **CE provides a principled approach to uncertainty quantification that operates at inference time without additional training.** Our experiments across diverse OCR scenarios demonstrate that CE-guided framework outperforms current vlm-as-judge methods but also enables practical strategies for quality filtering, prediction selection, and resource-efficient deployment. The simplicity and effectiveness of CE highlight how insights into model prediction patterns can lead to robust solutions for real-world challenges in document understanding. Future work could extend these principles to subjective vision-language tasks [13, 57] and incorporate the observed divergence patterns into upstream training methodologies [9]. Looking forward, CE opens promising research directions for uncertainty quantification and data routing strategies for VLM training dataset in multimodal large language models community.

REFERENCES

- [1] 1992. Historical review of OCR research and development. *Proc. IEEE* 80, 7 (1992), 1029–1058.
- [2] 2008–2025. GROBID. <https://github.com/kermitt2/grobid>. swb:1.dir:dab86b296e3c3216e2241968f0d63b68e8209d3c
- [3] Shuai Bai, Keqin Chen, Xuejing Liu, Jialin Wang, Wenbin Ge, Sibao Song, Kai Dang, Peng Wang, Shijie Wang, Jun Tang, Humen Zhong, Yuanzhi Zhu, Mingkun Yang, Zhaohai Li, Jianqiang Wan, Pengfei Wang, Wei Ding, Zheren Fu, Yiheng Xu, Jiabo Ye, Xi Zhang, Tianbao Xie, Zesen Cheng, Hang Zhang, Zhibo Yang, Haiyang Xu, and Junyang Lin. 2025. Qwen2.5-VL Technical Report. *arXiv preprint arXiv:2502.13923* (2025).
- [4] Tim Beyer, Sophie Xhonneux, Simon Geisler, Gauthier Gidel, Leo Schwinn, and Stephan Günnemann. 2025. LLM-Safety Evaluations Lack Robustness. *arXiv:2503.02574* [cs.CR] <https://arxiv.org/abs/2503.02574>
- [5] Lukas Blecher, Guillem Cucurull, Thomas Scialom, and Robert Stojnic. 2024. Nougat: Neural Optical Understanding for Academic Documents. *arXiv:2308.13418* (2024).
- [6] Yupeng Chang, Xu Wang, Jindong Wang, Yuan Wu, Linyi Yang, Kaijie Zhu, Hao Chen, Xiaoyuan Yi, Cunxiang Wang, Yidong Wang, et al. 2024. A survey on evaluation of large language models. *ACM transactions on intelligent systems and technology* 15, 3 (2024), 1–45.
- [7] Kedi Chen, Qin Chen, Jie Zhou, Xinqi Tao, Bowen Ding, Jingwen Xie, Mingchen Xie, Peilong Li, Feng Zheng, and Liang He. 2025. Enhancing Uncertainty Modeling with Semantic Graph for Hallucination Detection. *arXiv preprint arXiv:2501.02020* (2025).
- [8] Liang Chen, Yang Deng, Yatao Bian, Zeyu Qin, and et al. 2023. Beyond Factuality: A Comprehensive Evaluation of Large Language Models as Knowledge Generators. In *EMNLP 2023*. Association for Computational Linguistics, 6325–6341. doi:10.18653/V1/2023.EMNLP-MAIN.390
- [9] Zhijun Chen, Jingzheng Li, Pengpeng Chen, Zhuoran Li, Kai Sun, Yuankai Luo, Qianren Mao, Dingqi Yang, Hailong Sun, and Philip S. Yu. 2025. Harnessing Multiple Large Language Models: A Survey on LLM Ensemble. *arXiv:2502.18036* [cs.CL] <https://arxiv.org/abs/2502.18036>
- [10] Zhe Chen, Weiyun Wang, Yue Cao, Yangzhou Liu, Zhangwei Gao, Erfei Cui, Jinguo Zhu, Shenglong Ye, Hao Tian, Zhaoyang Liu, et al. 2024. Expanding Performance Boundaries of Open-Source Multimodal Models with Model, Data, and Test-Time Scaling. *arXiv preprint arXiv:2412.05271* (2024).
- [11] Zhe Chen, Weiyun Wang, Hao Tian, Shenglong Ye, Zhangwei Gao, Erfei Cui, Wenwen Tong, Kongzhi Hu, Jiapeng Luo, Zheng Ma, et al. 2024. How far are we to gpt-4v? closing the gap to commercial multimodal models with open-source suites. *Science China Information Sciences* 67, 12 (2024), 220101.
- [12] Wenliang Dai, Nayeon Lee, Boxin Wang, Zhuolin Yang, Zihan Liu, Jon Barker, Tuomas Rintamaki, Mohammad Shoeybi, Bryan Catanzaro, and Wei Ping. 2024. NVLM: Open Frontier-Class Multimodal LLMs. *arXiv:2409.11402* [cs.CL] <https://arxiv.org/abs/2409.11402>
- [13] Seyed Pouyan Mousavi Davoudi, Alireza Shafiee Fard, and Alireza Amiri-Margavi. 2025. Collective Reasoning Among LLMs A Framework for Answer Validation Without Ground Truth. *arXiv:2502.20758* [stat.AP] <https://arxiv.org/abs/2502.20758>
- [14] Haodong Duan, Junming Yang, Yuxuan Qiao, Xinyu Fang, Lin Chen, Yuan Liu, Xiaoyi Dong, Yuhang Zang, Pan Zhang, Jiaqi Wang, et al. 2024. Vlmevalkit: An open-source toolkit for evaluating large multi-modality models. In *Proceedings of the 32nd ACM International Conference on Multimedia*. 11198–11201.
- [15] Ling Fu, Biao Yang, Zhebin Kuang, Jiajun Song, Yuzhe Li, Linghao Zhu, Qidi Luo, Xinyu Wang, Hao Lu, Mingxin Huang, Zhang Li, Guozhi Tang, Bin Shan, Chunhui Lin, Qi Liu, Binghong Wu, Hao Feng, Hao Liu, Can Huang, Jingqun Tang, Wei Chen, Lianwen Jin, Yuliang Liu, and Xiang Bai. 2024. OCRBench v2: An Improved Benchmark for Evaluating Large Multimodal Models on Visual Text Localization and Reasoning. *arXiv:2501.00321* [cs.CV] <https://arxiv.org/abs/2501.00321>
- [16] Yarin Gal and Zoubin Ghahramani. 2016. Dropout as a bayesian approximation: Representing model uncertainty in deep learning. In *international conference on machine learning*. PMLR, 1050–1059.
- [17] Zhangwei Gao, Zhe Chen, Erfei Cui, Yiming Ren, Weiyun Wang, Jinguo Zhu, Hao Tian, Shenglong Ye, Junjun He, Xizhou Zhu, et al. 2024. Mini-InternVL: a flexible-transfer pocket multi-modal model with 5% parameters and 90% performance. *Visual Intelligence* 2, 1 (2024), 1–17.
- [18] Team GLM, Aohan Zeng, Bin Xu, Bowen Wang, Chenhui Zhang, Da Yin, Diego Rojas, Guanyu Feng, Hanlin Zhao, Hanyu Lai, Hao Yu, Hongning Wang, Jiadai Sun, Jiajie Zhang, Jiale Cheng, Jiayi Gui, Jie Tang, Jing Zhang, Juanzi Li, Lei Zhao, Lindong Wu, Lucen Zhong, Mingdao Liu, Minlie Huang, Peng Zhang, Qinkai Zheng, Rui Lu, Shuaiqi Duan, Shudan Zhang, Shulin Cao, Shuxun Yang, Weng Lam Tam, Wenyi Zhao, Xiao Liu, Xiao Xia, Xiaohan Zhang, Xiaotao Gu, Xin Lv, Xinghan Liu, Xinyi Liu, Xinyue Yang, Xixuan Song, Xunkai Zhang, Yifan An, Yifan Xu, Yilin Niu, Yuantao Yang, Yueyan Li, Yushi Bai, Yuxiao Dong, Zehan Qi, Zhaoyu Wang, Zhen Yang, Zhengxiao Du, Zhenyu Hou, and Zihan Wang. 2024. ChatGLM: A Family of Large Language Models from GLM-130B to GLM-4 All Tools.
- [19] Jiawei Gu, Xuhui Jiang, Zhichao Shi, Hexiang Tan, Xuehao Zhai, Chengjin Xu, Wei Li, Yinghan Shen, Shengjie Ma, Honghao Liu, et al. 2024. A Survey on LLM-as-a-Judge. *arXiv preprint arXiv:2411.15594* (2024).
- [20] Neel Guha, Mayee F Chen, Trevor Chow, Ishan S Khare, and Christopher Re. 2024. Smoothie: Label Free Language Model Routing. In *NeuIPS*.
- [21] Conghui He, Wei Li, Zhenjiang Jin, Chao Xu, Bin Wang, and Dahua Lin. 2024. Opendatalab: Empowering general artificial intelligence with open datasets. *arXiv preprint arXiv:2407.13773* (2024).
- [22] Conghui He, Wei Li, Zhenjiang Jin, Chao Xu, Bin Wang, and Dahua Lin. 2024. Opendatalab: Empowering general artificial intelligence with open datasets. *arXiv preprint arXiv:2407.13773* (2024).
- [23] Yupan Huang, Tengchao Lv, Lei Cui, Yutong Lu, and Furu Wei. 2022. Layoutlmv3: Pre-training for document ai with unified text and image masking. In *Proceedings of the 30th ACM international conference on multimedia*. 4083–4091.
- [24] Yuheng Huang, Jiayang Song, Zhijie Wang, Huaming Chen, and Lei Ma. 2023. Look Before You Leap: An Exploratory Study of Uncertainty Measurement for Large Language Models. *CoRR* abs/2307.10236 (2023). doi:10.48550/ARXIV.2307.10236
- [25] Metod Jazbec, Eliot Wong-Toi, Guoxuan Xia, Dan Zhang, Eric Nalisnick, and Stephan Mandt. 2025. Generative Uncertainty in Diffusion Models. *arXiv:2502.20946* [cs.LG] <https://arxiv.org/abs/2502.20946>
- [26] Dongfu Jiang, Xiang Ren, and Bill Yuchen Lin. 2023. LLM-Blender: Ensembling Large Language Models with Pairwise Ranking and Generative Fusion. In *ACL*.
- [27] Alex Kendall and Yarin Gal. 2017. What uncertainties do we need in bayesian deep learning for computer vision? *Advances in neural information processing systems* 30 (2017).
- [28] Seungone Kim, Jamin Shin, Yejin Cho, Joel Jang, Shayne Longpre, Hwaran Lee, Sangdoon Yun, Seongjin Shin, Sungdong Kim, James Thorne, et al. 2023. Prometheus: Inducing fine-grained evaluation capability in language models. In *The Twelfth International Conference on Learning Representations*.
- [29] Woosuk Kwon, Zhuohan Li, Siyuan Zhuang, Ying Sheng, Lianmin Zheng, Cody Hao Yu, Joseph E. Gonzalez, Hao Zhang, and Ion Stoica. 2023. Efficient Memory Management for Large Language Model Serving with PagedAttention. In *Proceedings of the ACM SIGOPS 29th Symposium on Operating Systems Principles*.
- [30] Dawei Li, Renliang Sun, Yue Huang, Ming Zhong, Bohan Jiang, Jiawei Han, Xiangliang Zhang, Wei Wang, and Huan Liu. 2025. Preference Leakage: A Contamination Problem in LLM-as-a-judge. *arXiv:2502.01534* [cs.LG] <https://arxiv.org/abs/2502.01534>
- [31] Junyuo Li, Qin Zhang, Yangbin Yu, Qiang Fu, and Deheng Ye. 2024. More agents is all you need. *arXiv preprint arXiv:2402.05120* (2024).
- [32] Yifan Li, Yifan Du, Kun Zhou, Jimpeng Wang, Xin Zhao, and Ji-Rong Wen. [n. d.]. Evaluating Object Hallucination in Large Vision-Language Models. In *The 2023 Conference on Empirical Methods in Natural Language Processing*.
- [33] Chin-Yew Lin. 2004. ROUGE: A Package for Automatic Evaluation of Summaries. In *Text Summarization Branches Out*. Association for Computational Linguistics, Barcelona, Spain, 74–81. <https://aclanthology.org/W04-1013/>
- [34] Chenglong Liu, Haoran Wei, Jinyue Chen, Lingyu Kong, Zheng Ge, Zining Zhu, Liang Zhao, Jianjian Sun, Chunrui Han, and Xiangyu Zhang. 2024. Focus Anywhere for Fine-grained Multi-page Document Understanding. *arXiv:2405.14295* (2024).
- [35] Haotian Liu, Chunyuan Li, Qingyang Wu, and Yong Jae Lee. 2023. Visual Instruction Tuning.
- [36] Xiaoou Liu, Tiejun Chen, Longchao Da, Chacha Chen, Zhen Lin, and Hua Wei. 2025. Uncertainty Quantification and Confidence Calibration in Large Language Models: A Survey. *arXiv:2503.15850* [cs.CL] <https://arxiv.org/abs/2503.15850>
- [37] Yuliang Liu, Zhang Li, Mingxin Huang, Biao Yang, Wenwen Yu, Chunyuan Li, Xu-Cheng Yin, Cheng-Lin Liu, Lianwen Jin, and Xiang Bai. 2024. OCRBench: on the hidden mystery of OCR in large multimodal models. *Science China Information Sciences* 67, 12 (Dec. 2024). doi:10.1007/s11432-024-4235-6
- [38] Yuxuan Liu, Tianchi Yang, Shaohan Huang, Zihan Zhang, Haizhen Huang, Furu Wei, Weiwei Deng, Feng Sun, and Qi Zhang. 2024. Calibrating LLM-Based Evaluator. In *Proceedings of the 2024 Joint International Conference on Computational Linguistics, Language Resources and Evaluation (LREC-COLING 2024)*. 2638–2656.
- [39] Shiyin Lu, Yang Li, Qing-Guo Chen, Zhao Xu, Weihua Luo, Kaifu Zhang, and Han-Jia Ye. 2024. Ovis: Structural Embedding Alignment for Multimodal Large Language Model. *arXiv:2405.20797* (2024).
- [40] Bo Lv, Chen Tang, Yanan Zhang, Xin Liu, Ping Luo, and Yue Yu. 2024. URG: A Unified Ranking and Generation Method for Ensembling Language Models. In *Findings of the ACL*.
- [41] Potsawee Manakul, Adian Liusie, and Mark J. F. Gales. 2023. SelfCheckGPT: Zero-Resource Black-Box Hallucination Detection for Generative Large Language Models. In *EMNLP 2023*. Association for Computational Linguistics, 9004–9017. doi:10.18653/V1/2023.EMNLP-MAIN.557
- [42] OpenAI. 2024. GPT-4o Technical Overview. <https://openai.com/index/gpt-4o-system-card/>. Accessed: 2025-04-06.
- [43] Kishore Papineni, Salim Roukos, Todd Ward, and Wei-Jing Zhu. 2002. Bleu: a method for automatic evaluation of machine translation. In *Proceedings of the*

- 40th annual meeting of the Association for Computational Linguistics. 311–318.
- [44] Felix Petersen, Aashwin Mishra, Hilde Kuehne, Christian Borgelt, Oliver Deussen, and Mikhail Yurochkin. 2024. Uncertainty Quantification via Stable Distribution Propagation. arXiv:2402.08324 [cs.LG] <https://arxiv.org/abs/2402.08324>
- [45] Jake Poznanski, Jon Borchardt, Jason Dunkelberger, Regan Huff, Daniel Lin, Aman Rangapur, Christopher Wilhelm, Kyle Lo, and Luca Soldaini. 2025. olmOCR: Unlocking Trillions of Tokens in PDFs with Vision Language Models. arXiv:2502.18443 [cs.CL] <https://arxiv.org/abs/2502.18443>
- [46] Javier Rando, Jie Zhang, Nicholas Carlini, and Florian Tramèr. 2025. Adversarial ML Problems Are Getting Harder to Solve and to Evaluate. arXiv:2502.02260 [cs.LG] <https://arxiv.org/abs/2502.02260>
- [47] Sense. 2025. SenseChat-Vision. <https://lobechat.com/discover/model/SenseChat-5?hl=zh-CN>.
- [48] Zejiang Shen, Kyle Lo, Lucy Lu Wang, Bailey Kuehl, Daniel S Weld, and Doug Downey. 2022. VILA: Improving structured content extraction from scientific PDFs using visual layout groups. *Transactions of the Association for Computational Linguistics* 10 (2022), 376–392.
- [49] Shopee-MUG. 2024. MUG-U. <https://github.com/Shopee-MUG/MUG-U>.
- [50] Chenglei Si, Weijia Shi, Chen Zhao, Luke Zettlemoyer, and Jordan Boyd-Graber. 2023. Getting MoRE out of Mixture of Language Model Reasoning Experts. In *Findings of EMNLP*.
- [51] Aarohi Srivastava, Abhinav Rastogi, Abhishek Rao, Abu Awal Md Shueb, Abubakar Abid, Adam Fisch, Adam R Brown, Adam Santoro, Aditya Gupta, Adrià Garriga-Alonso, et al. 2022. Beyond the imitation game: Quantifying and extrapolating the capabilities of language models. *arXiv preprint arXiv:2206.04615* (2022).
- [52] stepfun. 2024. Step-1V. <https://platform.stepfun.com/docs/llm/vision>.
- [53] Selim Tekin, Fatih Ilhan, Tiansheng Huang, Sihao Hu, and Ling Liu. 2024. LLM-TOPLA: Efficient LLM Ensemble by Maximising Diversity. In *Findings of EMNLP*.
- [54] Bin Wang, Chao Xu, Xiaomeng Zhao, Linke Ouyang, Fan Wu, Zhiyuan Zhao, Rui Xu, Kaiwen Liu, Yuan Qu, Fukai Shang, Bo Zhang, Liqun Wei, Zhihao Sui, Wei Li, Botian Shi, Yu Qiao, Dahua Lin, and Conghui He. 2024. MinerU: An Open-Source Solution for Precise Document Content Extraction. arXiv:2409.18839 [cs.CV] <https://arxiv.org/abs/2409.18839>
- [55] Bin Wang, Chao Xu, Xiaomeng Zhao, Linke Ouyang, Fan Wu, Zhiyuan Zhao, Rui Xu, Kaiwen Liu, Yuan Qu, Fukai Shang, Bo Zhang, Liqun Wei, Zhihao Sui, Wei Li, Botian Shi, Yu Qiao, Dahua Lin, and Conghui He. 2024. MinerU: An Open-Source Solution for Precise Document Content Extraction. arXiv:2409.18839 [cs.CV] <https://arxiv.org/abs/2409.18839>
- [56] Peng Wang, Shuai Bai, Sinan Tan, Shijie Wang, Zhihao Fan, Jinze Bai, Keqin Chen, Xuejing Liu, Jialin Wang, Wenbin Ge, Yang Fan, Kai Dang, Mengfei Du, Xuancheng Ren, Rui Men, Dayiheng Liu, Chang Zhou, Jingren Zhou, and Junyang Lin. 2024. Qwen2-VL: Enhancing Vision-Language Model’s Perception of the World at Any Resolution. *arXiv preprint arXiv:2409.12191* (2024).
- [57] Yiming Wang, Pei Zhang, Baosong Yang, Derek F Wong, and Rui Wang. 2024. Latent Space Chain-of-Embedding Enables Output-free LLM Self-Evaluation. *arXiv preprint arXiv:2410.13640* (2024).
- [58] Haoran Wei, Chenglong Liu, Jinyue Chen, Jia Wang, Lingyu Kong, Yanming Xu, Zheng Ge, Liang Zhao, Jianjian Sun, Yuang Peng, et al. 2024. General ocr theory: Towards ocr-2.0 via a unified end-to-end model. *arXiv:2409.01704* (2024).
- [59] Miao Xiong, Zhiyuan Hu, Xinyang Lu, YIFEI LI, Jie Fu, Junxian He, and Bryan Hooi. 2024. Can LLMs Express Their Uncertainty? An Empirical Evaluation of Confidence Elicitation in LLMs. In *The Twelfth International Conference on Learning Representations*. <https://openreview.net/forum?id=gjeQKfXpZ>
- [60] Zhong Xu, Jianbin Tang, and Antonio Jimeno Yepes. 2019. Publaynet: largest dataset ever for document layout analysis. In *2019 International conference on document analysis and recognition*. 1015–1022.
- [61] Zhibo Yang, Jun Tang, Zhaohai Li, Pengfei Wang, Jianqiang Wan, Humen Zhong, Xuejing Liu, Mingkun Yang, Peng Wang, Shuai Bai, LianWen Jin, and Junyang Lin. 2024. CC-OCR: A Comprehensive and Challenging OCR Benchmark for Evaluating Large Multimodal Models in Literacy. arXiv:2412.02210 [cs.CV] <https://arxiv.org/abs/2412.02210>
- [62] Yuan Yao, Tianyu Yu, Ao Zhang, Chongyi Wang, Junbo Cui, Hongji Zhu, Tianchi Cai, Haoyu Li, Weilin Zhao, Zhihui He, et al. 2024. MiniCPM-V: A GPT-4V Level MLLM on Your Phone. *arXiv preprint arXiv:2408.01800* (2024).
- [63] Ruiyang Zhang, Hu Zhang, and Zhedong Zheng. 2024. VL-Uncertainty: Detecting Hallucination in Large Vision-Language Model via Uncertainty Estimation. arXiv:2411.11919 [cs.CV] <https://arxiv.org/abs/2411.11919>
- [64] Lianmin Zheng, Wei-Lin Chiang, Ying Sheng, Siyuan Zhuang, Zhanghao Wu, Yonghao Zhuang, Zi Lin, Zhuohan Li, Dacheng Li, Eric Xing, et al. 2023. Judging llm-as-a-judge with mt-bench and chatbot arena. *Advances in Neural Information Processing Systems* 36 (2023), 46595–46623.
- [65] Lianghui Zhu, Xinggang Wang, and Xinlong Wang. 2023. JudgeLM: Fine-tuned Large Language Models are Scalable Judges. (2023). arXiv:2310.17631 [cs.CL]

We provide more details of the proposed method and additional experimental results to help better understand our paper. The appendix is organized to present comprehensive information on our experimental setup, prompting strategies, additional results, and limitations of the current approach.

Contents

A	Experiment Setting	11
B	Experimental Configuration	11
C	OCR Evaluation Case Studies	11
D	Prompt	11
D.1	Evaluation Metrics	14
D.2	Details of Compared Methods	15
E	Additional Experimental Results	15
E.1	Comparative Analysis of OCR Methods	15
E.2	Average Scores of 3 models on OCRBench-V2 under Different CE Thresholds. It shows CE is still effective in verifying OCR tasks of other benchmark, even some Visual Question Answering (VQA) tasks	16
F	RealData Source Composition	17
G	Annotation Interface for Human Evaluation	18
H	Algorithm Details	19
I	Ensemble Results	19
I.1	CCOCR	19
I.2	OCRBench-V2	19
I.3	OCRBench	20
J	Limitations and Future Directions	32

A EXPERIMENT SETTING

The version of GPT4o in this paper is "gpt-4o-2024-11-20".

B EXPERIMENTAL CONFIGURATION

Our experimental framework was carefully designed to ensure robust evaluation of the Consensus Entropy metric across diverse OCR scenarios. We employed a standardized computing environment with NVIDIA A100 GPUs for all model inference tasks. To maintain methodological consistency, we adopted the environmental settings established in vlmevalkit for VLM evaluations. All models were run with their default hyperparameters as specified in their original implementations, with the exception of temperature settings, which were standardized at 0.7 across all models to ensure fair comparison. The batch size was adjusted based on model size to optimize for both computational efficiency and memory constraints, with larger models using smaller batch sizes. Data preprocessing followed identical protocols across all experiments, with images normalized to a standard resolution while preserving aspect ratios. This configuration ensured that performance differences could be attributed to algorithmic distinctions rather than implementation variations.

C OCR EVALUATION CASE STUDIES

To provide a more intuitive understanding of how Consensus Entropy (CE) compares with VLM-as-Judge methods in real-world OCR tasks, we present several representative cases that highlight their respective performance characteristics.

These cases demonstrate that both CE and VLM-as-Judge methods generally align with human evaluation, but with important differences. CE shows particularly strong correlation with human judgments on complex documents (Cases 1, 3, and 5), where nuanced understanding is required. The strong agreement between human scores and automated methods validates our approach, particularly the training-free CE method which achieves comparable performance to supervised VLM-as-Judge approaches without requiring explicit quality assessment prompting.

Notably, in cases with clear quality issues (Case 2), both methods accurately identify poor OCR results, confirming their reliability for quality filtering applications. For structured content (Case 4), both approaches excel, suggesting that format preservation is well-captured by these evaluation techniques.

These qualitative examples complement our quantitative results in Section 4, reinforcing that CE provides a robust, unsupervised alternative to more complex and computationally expensive VLM-as-Judge methods for OCR quality assessment.

D PROMPT

The effectiveness of OCR tasks in VLLMs is significantly influenced by the design of prompts. We present the primary prompts utilized in our experiments below, each serving a specific purpose in the evaluation framework. These prompts were carefully crafted based on extensive preliminary explorations to maximize OCR performance while maintaining consistency across different models.

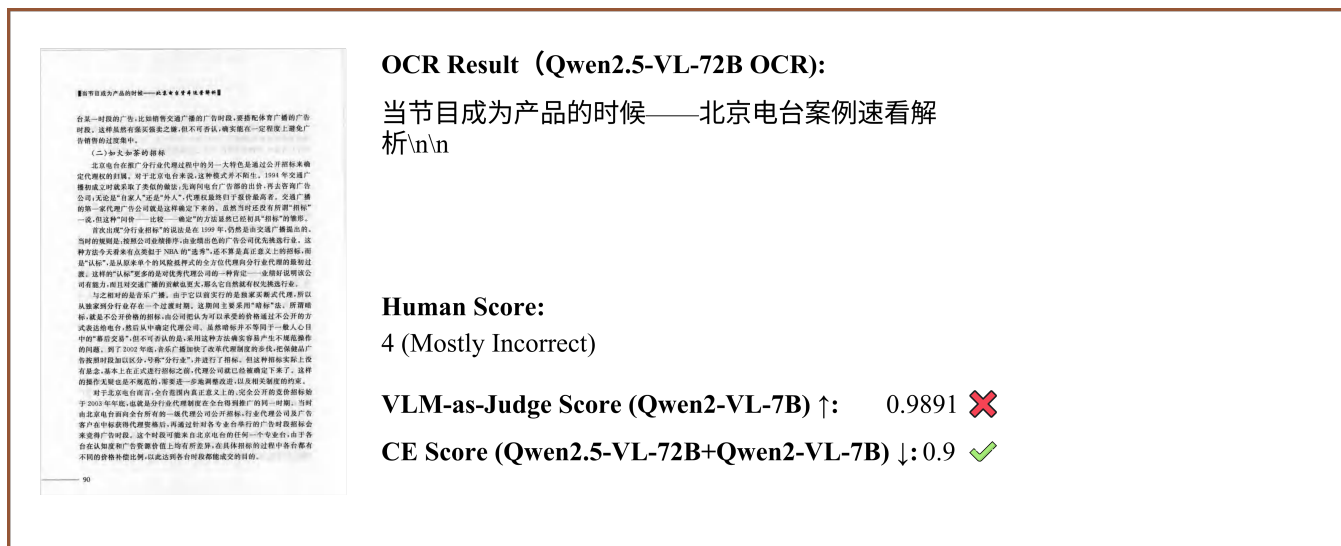


Figure 6: Case 1: High-quality Chinese OCR sample with strong agreement between human evaluation (4/4), CE score (0.9891), and VLM-as-Judge score (0.9).

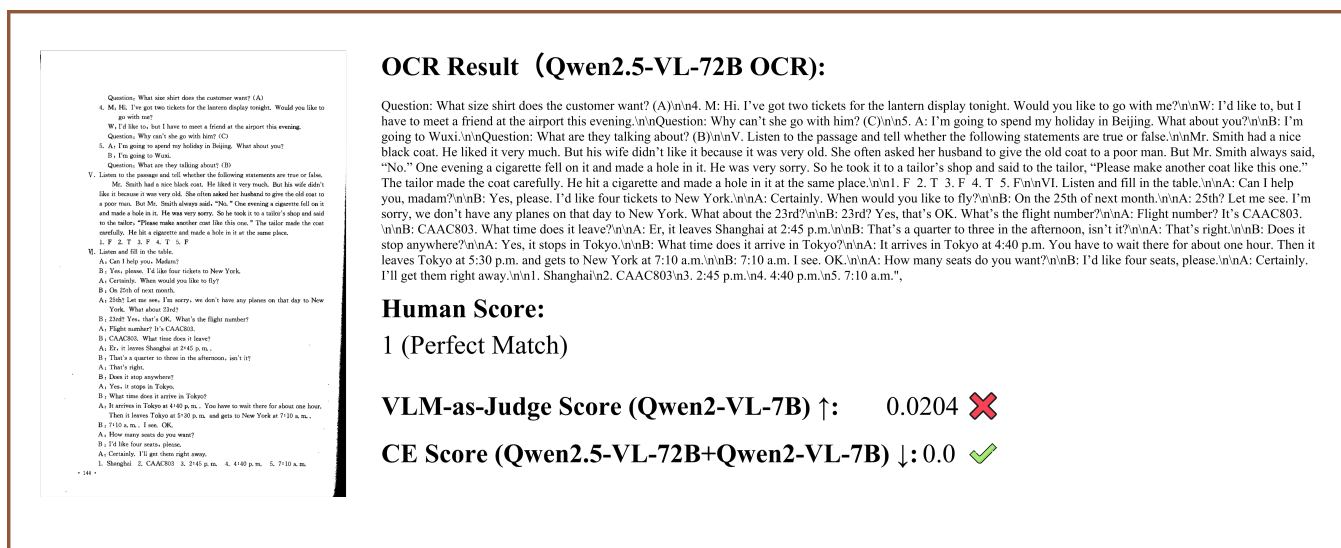


Figure 7: Case 2: Low-quality English OCR sample with unanimous poor quality assessment across human evaluation (1/4), CE score (0.0204), and VLM-as-Judge score (0.0).

OCR VLM-as-Judge Prompt

You are an expert evaluator assessing the quality of OCR (Optical Character Recognition) model predictions.

You will receive:

- A question
- A prediction generated by the OCR model.
- The corresponding image containing text.

Your task is to judge how well the predicted text matches the visual textual content in the image, with respect to the question's intent.

Evaluation criteria:

- (1) Focus only on whether the prediction correctly reflects the textual content of the image.
- (2) Assign a score from 0 to 1 in steps of 0.1, using the following four-level guideline:

Scoring Reference:

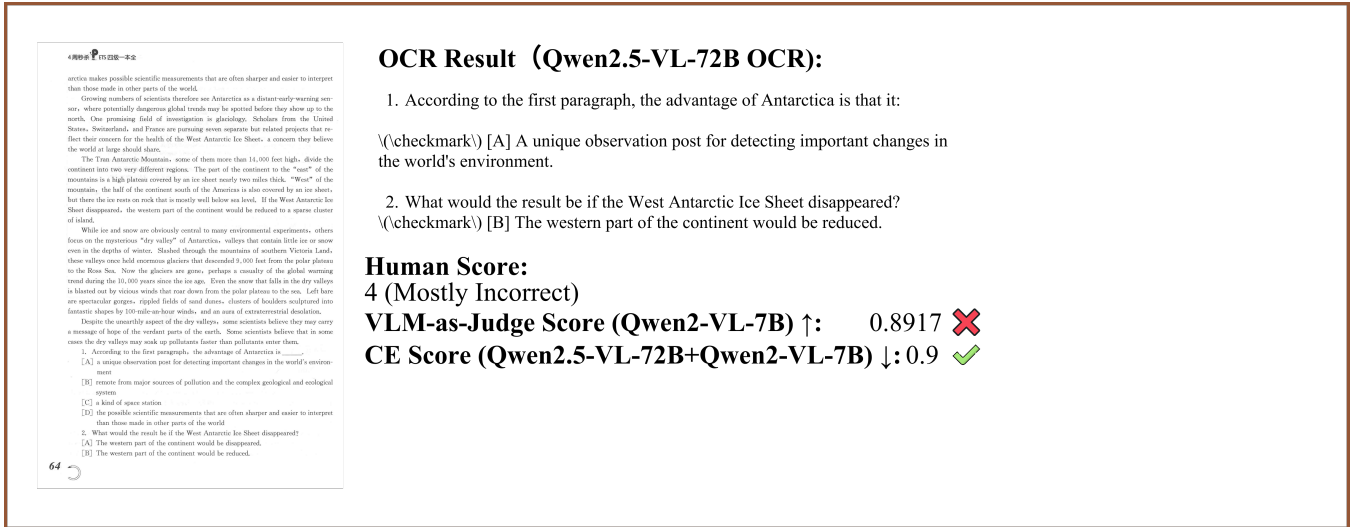


Figure 10: Case 5: Multiple-choice test questions accurately evaluated by all methods, showing robust performance on educational content with specialized formatting.

OCR CE-Guided Router Prompt

You are an expert AI assistant tasked with improving answers to visual questions. Please look at the image and examine the following question and the current answers from different models.

Question: {question}

Current model predictions: {predictions_str}

Your task is to synthesize these predictions and create a single improved answer that:

- (1) Is more accurate based on the visual content
- (2) Is concise and direct
- (3) Uses a natural, conversational tone
- (4) Maintains the core meaning of the original answers if they were correct
- (5) Improves clarity and precision

Do not invent details not present in the image. Your answer should be grounded in what is actually visible. Please provide ONLY the improved answer with no explanations or additional text.

OCR Qwen2.5VL-72B Prompt

You are a very professional expert at OCR tasks. Please analyze the following image and extract all text content.

- (1) Ensure that the extracted text matches the original in the image and maintains the original structure.
- (2) If the image contains two columns, you should extract all text in the left column before you move on to the right.
- (3) Ignore the headers, but keep the footnotes, title.
- (4) You could either use LaTeX, KaTeX or Markdown format for math formulas, physics equations, chemical expressions etc.
- (5) Do not add or modify the original content!

D.1 Evaluation Metrics

To evaluate model performance, we employed multiple metrics assessing various aspects of OCR quality. The character error rate (CER) and word error rate (WER) measured the character-level and word-level accuracy respectively, capturing fine-grained recognition performance. BLEU and ROUGE-L scores assessed the overall textual similarity between predictions and ground truth, with ROUGE-L particularly sensitive to longer n-gram overlaps that indicate structural preservation. For semantic accuracy, we calculated embedding similarity using sentence transformers, which effectively captures meaning preservation even when exact wording differs. Additionally, we employed task-specific metrics for specialized OCR applications: formula recognition used a LaTeX-aware F1 score that accounts for equivalent expressions, while table extraction was evaluated using TEDS (Table Edit Distance Similarity) to measure structural fidelity. Collectively, these metrics provided a comprehensive evaluation framework that assessed both the syntactic accuracy and semantic fidelity of OCR outputs across diverse document understanding scenarios.

D.2 Details of Compared Methods

Our comparative analysis incorporated several state-of-the-art approaches for OCR evaluation and improvement. The VLM-as-Judge paradigm was implemented using three different foundation models: GPT4o, Qwen2-VL-72B, and Qwen2-VL-7B, each prompted with the standardized evaluation instructions shown in Section A.2. For traditional evaluation metrics, we utilized the benchmark methodology from OCRBench, employing exact match and fuzzy matching criteria with standardized preprocessing to normalize formatting variations. The self-verification methods included both the token-level confidence based approach and our proposed Consensus Entropy framework. For token-level confidence, we aggregated model-reported logit scores and calibrated them using temperature scaling. The CE framework was implemented with multiple variations in entropy calculation methods, including Mean Distance, Sum, Max, and Mean methods as detailed in Section 3.1 of the main paper. All baseline methods were evaluated using identical test samples and environmental configurations to ensure fair comparison.

E ADDITIONAL EXPERIMENTAL RESULTS

This section presents additional detailed analyses of our Consensus Entropy framework to complement the results discussed in the main paper. The extended results provide deeper insights into the behavior and effectiveness of different entropy calculation methods, the impact of distribution characteristics, and practical implications for deployment.

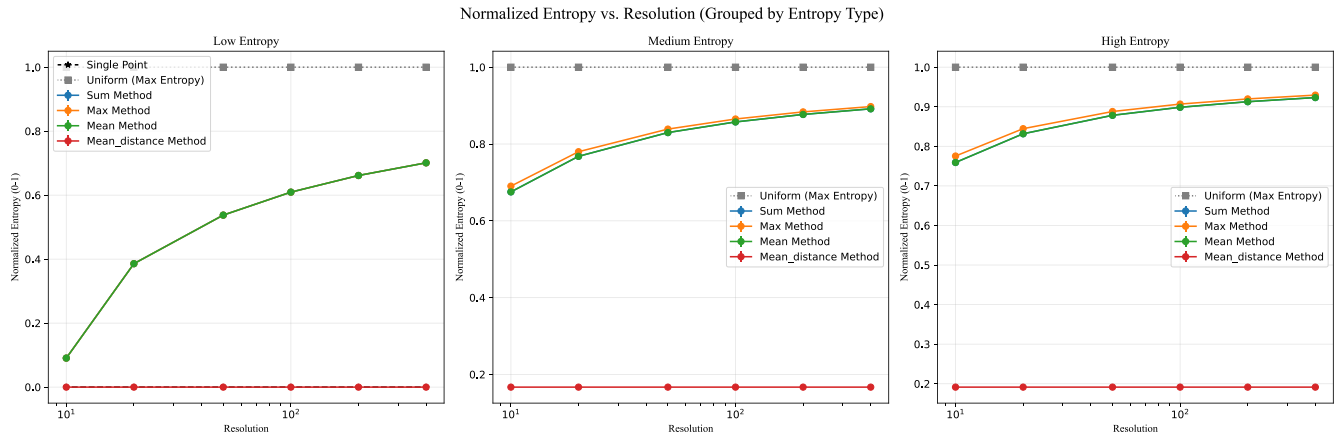


Figure 11: Normalized entropy comparison across different distribution types using the same aggregation methods. While Mean Distance shows the most distinctive pattern, all methods maintain similar relative positioning across distribution types, confirming the robustness of the entropy-based approach regardless of the specific computation method chosen.

Figure 11 extends our analysis of different aggregation methods by comparing their behavior across identical distribution types. The results demonstrate that while Mean Distance exhibits the most distinctive entropy pattern, all methods maintain consistent relative entropy values across distribution types. This consistency further validates our entropy-based approach by showing that the qualitative rankings of uncertainty remain stable regardless of the specific aggregation method employed.

E.1 Comparative Analysis of OCR Methods

To provide a comprehensive evaluation of different OCR approaches, we conducted a detailed comparison of three main strategies: Self-Consistency (SC@3), Routing-based ensemble, and Single model performance. Table 7 presents the results of this analysis, highlighting the relative performance improvements of each method.

The results demonstrate several key findings: First, the Routing-based ensemble approach consistently outperforms both SC@3 and Single model methods, with the best routing configuration achieving a score of 922, representing an 8.2% improvement over the best single model performance. Second, while SC@3 shows potential for improvement (2.7% over baseline when using Qwen2-VL-72B), its average performance actually decreases by 2.8%, indicating high variance in its effectiveness. Third, the gap between average and best performance is smallest for the Routing method (15 points) compared to SC@3 (47 points) and Single models (36 points), suggesting more consistent and reliable performance across different configurations.

Figure 12 investigates how kernel bandwidth settings and the correlation between distributions affect entropy estimates. A key finding is that higher correlation values consistently produce lower entropy curves, indicating that tightly clustered predictions (as would be expected for correct OCR outputs) naturally result in lower entropy measurements. This property is precisely what enables our CE metric to effectively distinguish between high-confidence and low-confidence predictions.

Table 7: Performance comparison of different OCR methods based on cumulative scores. SC@3 represents Self-Consistency with 3 samples, Routing refers to the ensemble with rephrasing, and Single indicates individual model performance. Blue highlights indicate the best performance in each category, while green highlights mark the second best.

Method	Score	Improvement (%)
SC@3 (Average)	828	-2.8
SC@3 (Best: Qwen2-VL-72B)	875	2.7
Routing (Average)	907	6.5
Routing (Best: Qwen2.5-VL-72B)	922	8.2
Single (Average)	852	-
Single (Best: Qwen2-VL-72B)	888	-

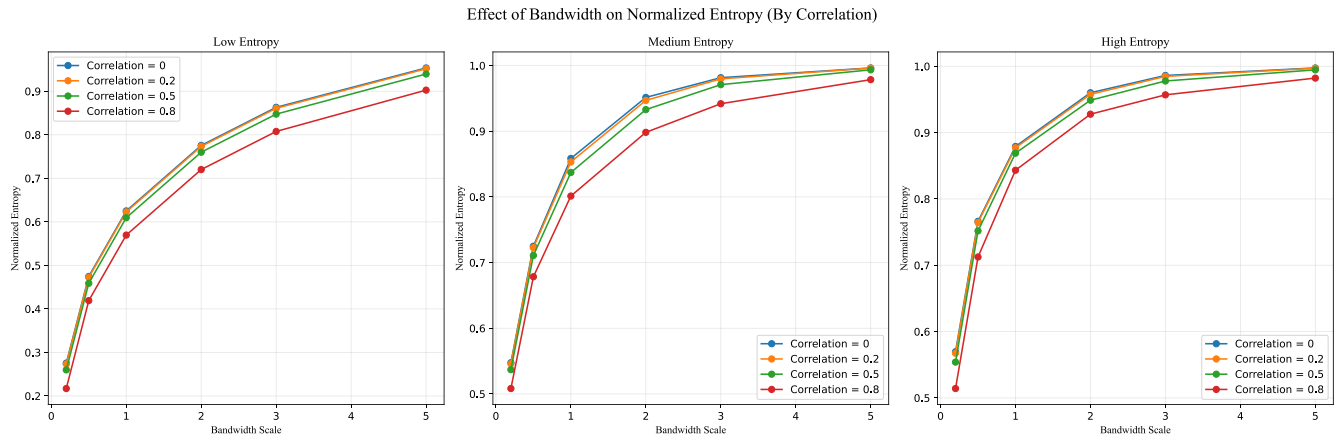


Figure 12: Effects of kernel bandwidth and distribution correlation on entropy estimates. Higher correlation values consistently result in lower entropy curves, highlighting how the spatial relationship between predictions influences the consensus measurement.

We also conducted experiments on OCRbench-V2 regarding the relationship between CE thresholds and benchmark scores, as shown in the 8

E.2 Average Scores of 3 models on OCRBench-V2 under Different CE Thresholds. It shows CE is still effective in verifying OCR tasks of other benchmark, even some Visual Question Answering (VQA) tasks

We also

Table 8: Performance of 3 models on OCRBench-V2 under Different CE Thresholds.

Model	CE Threshold	Total QAs	EN Overall	CN Overall	ALL Overall
Gemini-PRO	1.0	10000	0.519	0.431	0.520
	0.9	8816	0.549	0.465	0.546
	0.8	7252	0.580	0.535	0.582
	0.7	6009	0.614	0.560	0.610
	0.6	5221	0.643	0.588	0.633
	0.5	4499	0.640	0.596	0.652
	0.4	3276	0.702	0.650	0.668
	0.2	1664	0.785	0.648	0.743

Continued on next page

Table 8 – continued from previous page

Model	Threshold	Total Questions	EN Overall	CN Overall	ALL Overall
GPT4o	0.1	1041	0.828	0.690	0.790
	1.0	10000	0.465	0.322	0.473
	0.9	8357	0.521	0.394	0.541
	0.8	6571	0.559	0.463	0.584
	0.7	5341	0.585	0.529	0.604
	0.6	4566	0.595	0.581	0.615
	0.5	3903	0.614	0.625	0.639
	0.4	3031	0.652	0.647	0.652
	0.3	2423	0.665	0.708	0.682
	0.2	1665	0.769	0.663	0.736
Intern2.5VL-26B	0.1	1192	0.823	0.740	0.796
	1.0	10000	0.494	0.442	0.532
	0.9	7160	0.558	0.511	0.580
	0.8	5948	0.581	0.553	0.593
	0.7	5198	0.614	0.551	0.620
	0.6	4629	0.626	0.623	0.642
	0.5	3976	0.634	0.646	0.664
	0.4	2850	0.673	0.630	0.697
	0.3	2056	0.677	0.658	0.744
	0.2	1638	0.776	0.696	0.772
	0.1	1118	0.829	0.742	0.799

F REALDATA SOURCE COMPOSITION

The datasets used in our OCR evaluation experiments were carefully curated to reflect diverse real-world document scenarios. Below we present the detailed composition of these datasets, encompassing various languages, document types, and content domains.

Table 9: Sources of the OCR Dataset

	ebook	paper	textbook	other
ZH	zhishilei, zhongwenzaixian, gift, thomas	-	by, kps, kmath, zhonggaokao, gaojiaoshe, gaodengjiaoyu, k12 edu platform, jiaoan, zju icicles	-
EN	theeye, physicsandmathstutor, planetebook	escholarship, biorxiv, springer, sagepub, scholarworks, psyarxiv, chemrxiv, iop-science, royalsocietypublishing, criso	kps, bookboon, california 14sets, scholarworks	dev books repository
ML	renhang, banshujiang	-	openstax, math	-
Other	-	-	-	coursehero, studypool

The dataset composition encompasses a wide range of content types and sources, ensuring comprehensive evaluation of OCR capabilities. Chinese language materials include electronic books from major repositories as well as educational content across various academic levels. English content spans scholarly publications from multiple disciplines, educational materials, and literature. Multilingual resources incorporate specialized content with mixed language elements, while additional sources provide diverse formatting challenges. This heterogeneous collection enables robust assessment of OCR performance across domains, languages, and formatting complexities representative of real-world document processing requirements.

For human evaluation of OCR quality, we developed a standardized 4-level scoring system:

- (1) **Perfect Match (0.9-1.0)**: The prediction matches the image text exactly with no errors.
- (2) **Minor Errors (0.7-0.8)**: Very close to the image text with only small mistakes that do not affect understanding.
- (3) **Partially Correct (0.4-0.6)**: Contains noticeable errors or captures only part of the text.
- (4) **Mostly Incorrect (0.0-0.3)**: Largely incorrect or unrelated to the text in the image.

This scoring system was used consistently across all human evaluations in our experiments to ensure reliable assessment of OCR quality.

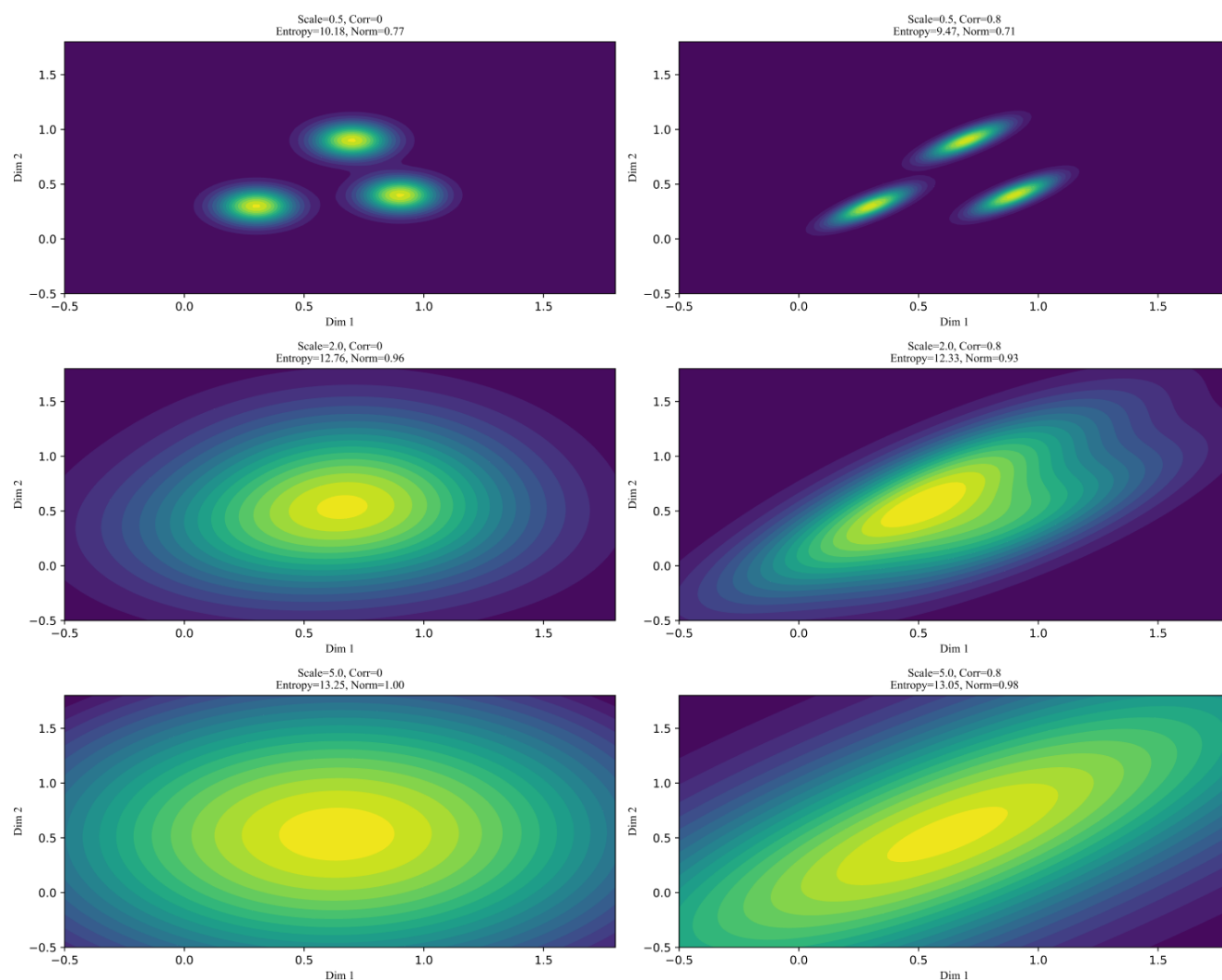


Figure 13: Visualization of entropy patterns across various scale and correlation settings. These examples illustrate how our entropy calculation responds to different distribution characteristics, with tighter, more correlated clusters resulting in lower entropy values regardless of scale.

G ANNOTATION INTERFACE FOR HUMAN EVALUATION

To ensure the quality of our real-world dataset and provide reliable human judgments for OCR performance evaluation, we developed a dedicated annotation interface. Figure 14 presents our custom-built tool designed specifically for OCR evaluation tasks.

The annotation interface is implemented using Gradio, a Python library for creating web-based interfaces. This tool facilitates efficient human evaluation of OCR results by displaying the original image alongside the extracted text. Annotators can assign one of four quality ratings to each OCR output: (1) Completely Correct, (2) Minor Errors, (3) Partially Correct, or (4) Mostly Incorrect. This standardized rating system ensures consistency across evaluations and provides fine-grained assessment of OCR quality.

The interface includes several features to enhance annotation efficiency: a status display showing progress through the dataset, navigation controls to move between samples, the ability to skip difficult cases, and a direct jump function to specific image indices. All annotations are automatically saved to the original data file, creating a persistent record of human judgments. This annotation tool played a critical role in developing our ground truth evaluations and validating the effectiveness of the Consensus Entropy framework against human quality assessments.

H ALGORITHM DETAILS

This section provides detailed pseudocode for the key algorithms used in our Consensus Entropy framework.

Algorithm 2 Consensus Entropy for Multi-Model OCR Evaluation

Require: $\{O_1, O_2, \dots, O_n\}$ - outputs from n OCR models for image I
Require: σ - base kernel bandwidth parameter
Require: α - adaptive bandwidth scaling factor
Require: N - grid resolution for probability density estimation
 // Compute pairwise entropies and weights
for $i = 1$ to n **do**
 for $j = 1$ to n , $j \neq i$ **do**
 $\mathcal{E}_{ij} \leftarrow \text{ComputePairwiseEntropy}(O_i, O_j)$
 end for
 $\bar{\mathcal{E}}_i \leftarrow \frac{1}{n-1} \sum_{j \neq i} \mathcal{E}_{ij}$ {Average entropy distance}
 $w_i \leftarrow \frac{1/\bar{\mathcal{E}}_i}{\sum_{k=1}^n 1/\bar{\mathcal{E}}_k}$ {Normalize weights}
 $\Sigma_i \leftarrow \sigma \cdot (1 + \alpha \cdot \bar{\mathcal{E}}_i) \cdot \mathbf{I}$ {Adaptive covariance}
end for
 // Project outputs to semantic space and estimate distribution on $N \times N$ grid
 $\{\mathbf{v}_1, \mathbf{v}_2, \dots, \mathbf{v}_n\} \leftarrow \text{ProjectToSemanticSpace}(\{O_1, O_2, \dots, O_n\})$
 $P \leftarrow \text{EstimateDistributionOnGrid}(\{\mathbf{v}_i, w_i, \Sigma_i\}_{i=1}^n, N)$
 // Calculate entropy from $N \times N$ grid-based distribution
 $\delta \leftarrow -\sum_{x=1}^N \sum_{y=1}^N P[x, y] \cdot \log P[x, y]$ {Discrete entropy calculation on $N \times N$ grid}
return δ {Return Consensus Entropy}

Algorithm 3 CE-OCR: Entropy-guided Ensemble and Routing Framework

Require: I - input image containing text
Require: $\{M_1, M_2, \dots, M_n\}$ - set of OCR models
Require: M_{exp} - stronger vision-language model for rephrasing
Require: θ - entropy threshold for routing
 $\{O_1, O_2, \dots, O_n\} \leftarrow \{M_1(I), M_2(I), \dots, M_n(I)\}$ {Generate predictions}
 $\delta \leftarrow \text{ConsensusEntropy}(\{O_1, O_2, \dots, O_n\})$ {Calculate entropy using Algorithm 1}
if $\delta \leq \theta$ **then**
 // Use precomputed weights from Algorithm 1
 $O_{\text{final}} \leftarrow \text{WeightedEnsemble}(\{O_1, O_2, \dots, O_n\}, \{w_1, w_2, \dots, w_n\})$
else
 $O_{\text{ens}} \leftarrow \text{SimpleEnsemble}(\{O_1, O_2, \dots, O_n\})$ {Basic ensemble}
 $O_{\text{final}} \leftarrow M_{\text{exp}}(I, \{O_1, O_2, \dots, O_n\}, O_{\text{ens}})$ {Route to stronger model for rephrasing}
end if
return O_{final}

I ENSEMBLE RESULTS

I.1 CCOCR

Table 10 summarizes the ensemble performance of three CE-selected model combinations on the CCOCR benchmark, spanning four major OCR task categories: *KIE*, *Document Parsing*, *Multilingual OCR*, and *Multi-scene OCR*. For each combination, we report both the ensemble results (first row) and the performance of the best-performing single model in the group (second row, *italicized*). The final column reports the *Overall Score*, computed as the average across the four tasks.

I.2 OCRBench-V2

Table 11 presents the bilingual evaluation of seven CE-selected multi-model aggregation schemes on OCRBench-V2. Each scheme combines four to five vision-language models (VLMs). *Ensemble Score* denotes the overall performance of the aggregated model, whereas *Single Best* is the highest-scoring individual model within the same ensemble for the corresponding language subset. Their absolute difference,

Table 10: CCOCR Ensemble Results

Models	Task Performance				Overall Score
	KIE	Doc Parsing	Multi Language	Multi Scene	
Qwen2.5-VL-3B, Qwen2.5-VL-7B, Qwen2.5-VL-72B	89.27	64.85	79.75	85.56	79.86
<i>Best Single (Qwen2.5-VL-72B)</i>	89.51	62.34	80.77	86.34	79.74
Qwen2.5-VL-3B, Qwen2.5-VL-7B, Qwen2-VL-7B-Instruct	87.16	61.19	77.49	83.09	77.23
<i>Best Single (Qwen2.5-VL-7B)</i>	87.42	60.67	78.49	84.12	77.67
InternVL2_5-4B, Qwen2.5-VL-7B, Qwen2.5-VL-72B	88.71	62.48	79.90	84.90	79.00
<i>Best Single (Qwen2.5-VL-72B)</i>	89.51	62.34	80.77	86.34	79.74

$\Delta = \text{Ensemble Score} - \text{Single Best}$, is reported in the right-most column. Results with the highest score in each language subset are highlighted in blue, and all positive gains ($\Delta > 0$) are shaded in green.

Table 11: OCRBench-V2 Ensemble Results

Models	Ensemble Score		Single Best		Δ	
	English	Chinese	English	Chinese	English	Chinese
internvl2 5 26b, qwen2vl-8b, gemini pro MiniCPM-V-2 6	0.588	0.528	0.555	0.442	0.033	0.086
gemini pro, gpt4o, internvl2 5 26b qwen2vl-8b	0.589	0.521	0.555	0.442	0.034	0.079
internvl2 5 26b, gpt4o, qwen2vl-8b MiniCPM-V-2 6	0.567	0.483	0.555	0.442	0.012	0.041
internvl2_8b, cambrian_8b, llava_onevision_qwen2_7b_ov	0.538	0.395	0.404	0.363	0.134	0.032
idefics3, llava_onevision_qwen2_7b_ov, MiniCPM-V-2_6	0.550	0.466	0.416	0.307	0.134	0.159
internvl2_8b, cambrian_8b, llavar	0.521	0.387	0.404	0.363	0.117	0.024
internvl2_8b, cambrian_8b, textharmony	0.520	0.394	0.404	0.363	0.116	0.031

I.3 OCRBench

Tables 12, 13, 14 present supplementary results on OCRBENCH, covering CE-selected ensemble combinations of 3, 4, and 5 models. Each row represents a specific ensemble configuration. The *Score* column reports the final ensemble performance obtained via CE-based prediction selection. The *Max*, *Min*, and *Avg* columns correspond to the highest, lowest, and mean scores among the participating individual models. The rightmost columns denote the absolute gains of the ensemble over its components: $\Delta_{\max} = \text{Score} - \text{Min}$, $\Delta_{\min} = \text{Score} - \text{Max}$, and $\Delta_{\text{avg}} = \text{Score} - \text{Avg}$. Blue highlights indicate the best result among both the ensemble and its constituent models, while green shading marks positive relative gains.

Table 12: OCRBench Ensemble Results (5 models)

Models	Score	Max	Min	Avg	Δ_{\max}	Δ_{\min}	Δ_{avg}
Ovis2-1B, Qwen2.5-VL-72B, SenseChat-Vision Step1V, Step1o	95.8	92.6	87.9	89.50	7.9	3.2	6.30
Ovis2-4B, Qwen2.5-VL-7B, SenseChat-Vision Step1V, Step1o	95.7	92.6	87.4	89.78	8.3	3.1	5.92
Ovis2-4B, Qwen2.5-VL-72B, SenseChat-Vision							

continued on next page

continuation sheet 12:OCRBench Ensemble Results (5 models)

Models	Score	Max	Min	Avg	Δ_{max}	Δ_{min}	Δ_{avg}
Step1V, Step1o	95.6	92.6	87.9	89.88	7.7	3.0	5.72
Ovis2-4B, Qwen-VL-Plus-0809, SenseChat-Vision Step1V, Step1o	95.6	92.6	84.3	89.16	11.3	3.0	6.44
MiniCPM-V-2_6, Qwen2.5-VL-72B, SenseChat-Vision Step1V, Step1o	95.6	92.6	85.2	88.74	10.4	3.0	6.86
Ovis2-1B, Qwen2.5-VL-7B, SenseChat-Vision Step1V, Step1o	95.5	92.6	87.4	89.40	8.1	2.9	6.10
Ovis2-4B, SenseChat-Vision, Step1V Step1o, bailingMM-Lite	95.5	92.6	85.2	89.34	10.3	2.9	6.16
GLM4V_PLUS, MUG-U-7B, Qwen2.5-VL-72B Step1V, Step1o	95.5	92.6	84.3	88.90	11.2	2.9	6.60
Ovis1.6-Gemma2-27B, Qwen2.5-VL-72B, SenseChat-Vision Step1V, Step1o	95.5	92.6	85.6	88.82	9.9	2.9	6.68
MUG-U-7B, Qwen2-VL-7B-Instruct, SenseChat-Vision Step1o, bailingMM-Lite	95.5	92.6	84.3	88.52	11.2	2.9	6.98
GLM4V_PLUS, Qwen2.5-VL-7B, SenseChat-Vision Step1V, Step1o	95.5	92.6	84.3	88.46	11.2	2.9	7.04
InternVL2_5-78B-MPO, Qwen2.5-VL-72B, SenseChat-Vision Step1V, Step1o	95.4	92.6	87.9	89.88	7.5	2.8	5.52
Ovis2-4B, Qwen2-VL-7B-Instruct, SenseChat-Vision Step1V, Step1o	95.4	92.6	84.3	89.16	11.1	2.8	6.24
Ovis2-4B, Qwen2-VL-7B-Instruct, Qwen2.5-VL-72B Step1V, Step1o	95.4	92.6	84.3	88.86	11.1	2.8	6.54
GLM4V_PLUS, Qwen2.5-VL-72B, SenseChat-Vision Step1V, Step1o	95.4	92.6	84.3	88.56	11.1	2.8	6.84
Ovis2-1B, Qwen2-VL-7B-Instruct, Qwen2.5-VL-72B Step1V, Step1o	95.4	92.6	84.3	88.48	11.1	2.8	6.92
MUG-U-7B, Ovis2-1B, Qwen2.5-VL-72B Step1V, Step1o	95.3	92.6	87.9	89.84	7.4	2.7	5.46
MUG-U-7B, Qwen2.5-VL-7B, SenseChat-Vision Step1V, Step1o	95.3	92.6	87.4	89.82	7.9	2.7	5.48
InternVL2_5-78B-MPO, Ovis2-1B, Qwen2.5-VL-72B Step1V, Step1o	95.3	92.6	87.9	89.80	7.4	2.7	5.50
MUG-U-7B, Ovis2-4B, Qwen-VL-Plus-0809 Step1V, Step1o	95.3	92.6	84.3	89.50	11.0	2.7	5.80
MUG-U-7B, Qwen2-VL-72B-Instruct, SenseChat-Vision Step1o, bailingMM-Lite	95.3	92.6	85.2	89.42	10.1	2.7	5.88
Ovis2-8B, SenseChat-Vision, Step1V Step1o, bailingMM-Lite	95.3	92.6	85.2	89.02	10.1	2.7	6.28
Ovis2-1B, Qwen-VL-Plus-0809, SenseChat-Vision Step1V, Step1o	95.3	92.6	84.3	88.78	11.0	2.7	6.52
Ovis2-1B, Qwen2-VL-7B-Instruct, SenseChat-Vision Step1V, Step1o	95.3	92.6	84.3	88.78	11.0	2.7	6.52
Qwen2.5-VL-72B, SenseChat-Vision, Step1V							

continued on next page

continuation sheet 12:OCRBench Ensemble Results (5 models)

Models	Score	Max	Min	Avg	Δ_{max}	Δ_{min}	Δ_{avg}
Step1o, bailingMM-Lite	95.3	92.6	85.2	88.74	10.1	2.7	6.56
MUG-U-7B, Qwen-VL-Plus-0809, SenseChat-Vision Step1o, bailingMM-Lite	95.3	92.6	84.3	88.52	11.0	2.7	6.78
GLM4V_PLUS, Ovis2-1B, Qwen2.5-VL-72B Step1V, Step1o	95.3	92.6	84.3	88.48	11.0	2.7	6.82
GLM4V_PLUS, MUG-U-7B, Qwen-VL-Plus-0809 Step1V, Step1o	95.3	92.6	84.3	88.18	11.0	2.7	7.12
MUG-U-7B, Ovis2-4B, Qwen2.5-VL-72B Step1V, Step1o	95.2	92.6	87.9	90.22	7.3	2.6	4.98
InternVL2_5-78B-MPO, Ovis2-1B, Qwen2.5-VL-7B Step1V, Step1o	95.2	92.6	87.4	89.70	7.8	2.6	5.50
MUG-U-7B, Qwen2-VL-72B-Instruct, Qwen2.5-VL-7B Step1V, Step1o	95.2	92.6	87.4	89.70	7.8	2.6	5.50
Ovis2-8B, Qwen2.5-VL-72B, SenseChat-Vision Step1V, Step1o	95.2	92.6	87.9	89.56	7.3	2.6	5.64
MUG-U-7B, Ovis2-4B, Qwen2-VL-7B-Instruct Step1V, Step1o	95.2	92.6	84.3	89.50	10.9	2.6	5.70
Ovis2-8B, Qwen2.5-VL-7B, SenseChat-Vision Step1V, Step1o	95.2	92.6	87.4	89.46	7.8	2.6	5.74
MUG-U-7B, SenseChat-Vision, Step1V Step1o, bailingMM-Lite	95.2	92.6	85.2	89.38	10.0	2.6	5.82
MUG-U-7B, Qwen2.5-VL-7B, SenseChat-Vision Step1o, bailingMM-Lite	95.2	92.6	85.2	89.14	10.0	2.6	6.06
MUG-U-7B, MiniCPM-V-2_6, Qwen2.5-VL-72B Step1V, Step1o	95.2	92.6	85.2	89.08	10.0	2.6	6.12
Ovis2-1B, SenseChat-Vision, Step1V Step1o, bailingMM-Lite	95.2	92.6	85.2	88.96	10.0	2.6	6.24
GLM4V_PLUS, MUG-U-7B, Qwen2.5-VL-7B Step1V, Step1o	95.2	92.6	84.3	88.80	10.9	2.6	6.40
Qwen2.5-VL-7B, SenseChat-Vision, Step1V Step1o, bailingMM-Lite	95.2	92.6	85.2	88.64	10.0	2.6	6.56
MiniCPM-V-2_6, Ovis2-1B, Qwen2.5-VL-7B Step1V, Step1o	95.2	92.6	85.2	88.56	10.0	2.6	6.64
Ovis2-1B, Qwen-VL-Plus-0809, Qwen2.5-VL-72B Step1V, Step1o	95.2	92.6	84.3	88.48	10.9	2.6	6.72
Qwen2-VL-7B-Instruct, SenseChat-Vision, Step1V Step1o, bailingMM-Lite	95.2	92.6	84.3	88.02	10.9	2.6	7.18
InternVL2_5-78B-MPO, MUG-U-7B, Qwen2.5-VL-72B Step1V, Step1o	95.1	92.6	87.9	90.22	7.2	2.5	4.88
MUG-U-7B, Ovis2-4B, Qwen2.5-VL-7B Step1V, Step1o	95.1	92.6	87.4	90.12	7.7	2.5	4.98
Ovis2-4B, Qwen2-VL-72B-Instruct, SenseChat-Vision Step1V, Step1o	95.1	92.6	88.6	90.06	6.5	2.5	5.04
InternVL2_5-78B-MPO, Qwen2.5-VL-7B, SenseChat-Vision							

continued on next page

continuation sheet 12:OCRBench Ensemble Results (5 models)

Models	Score	Max	Min	Avg	Δ_{max}	Δ_{min}	Δ_{avg}
Step1V, Step1o	95.1	92.6	87.4	89.78	7.7	2.5	5.32
MUG-U-7B, Ovis2-8B, Step1V Step1o, bailingMM-Lite	95.1	92.6	85.2	89.36	9.9	2.5	5.74
MUG-U-7B, Qwen-VL-Max-0809, SenseChat-Vision Step1o, bailingMM-Lite	95.1	92.6	85.2	89.28	9.9	2.5	5.82
MUG-U-7B, Qwen2.5-VL-72B, SenseChat-Vision Step1o, bailingMM-Lite	95.1	92.6	85.2	89.24	9.9	2.5	5.86
MUG-U-7B, Qwen2-VL-7B-Instruct, SenseChat-Vision Step1V, Step1o	95.1	92.6	84.3	89.20	10.8	2.5	5.90
Ovis2-4B, Ovis2-8B, Qwen2.5-VL-72B Step1o, bailingMM-Lite	95.1	92.6	85.2	89.18	9.9	2.5	5.92
MUG-U-7B, Ovis2-1B, Qwen-VL-Plus-0809 Step1V, Step1o	95.1	92.6	84.3	89.12	10.8	2.5	5.98
MUG-U-7B, Qwen-VL-Plus-0809, Qwen2-VL-72B-Instruct Step1V, Step1o	95.1	92.6	84.3	89.08	10.8	2.5	6.02
InternVL2_5-26B, Ovis2-1B, SenseChat-Vision Step1V, Step1o	95.1	92.6	85.4	89.00	9.7	2.5	6.10
Qwen2-VL-72B-Instruct, SenseChat-Vision, Step1V Step1o, bailingMM-Lite	95.1	92.6	85.2	88.92	9.9	2.5	6.18
InternVL2_5-38B, MUG-U-7B, Qwen2.5-VL-7B SenseChat-Vision, Step1o	95.1	92.6	84.1	88.92	11.0	2.5	6.18
Ovis2-4B, Qwen-VL-Plus-0809, Qwen2.5-VL-72B Step1V, Step1o	95.1	92.6	84.3	88.86	10.8	2.5	6.24
Ovis2-8B, Qwen-VL-Plus-0809, SenseChat-Vision Step1V, Step1o	95.1	92.6	84.3	88.84	10.8	2.5	6.26
Ovis2-8B, Qwen2-VL-7B-Instruct, SenseChat-Vision Step1V, Step1o	95.1	92.6	84.3	88.84	10.8	2.5	6.26
MUG-U-7B, Qwen2-VL-7B-Instruct, Qwen2.5-VL-7B Step1V, Step1o	95.1	92.6	84.3	88.80	10.8	2.5	6.30
InternVL2_5-38B, MUG-U-7B, Qwen2.5-VL-7B Step1V, Step1o	95.1	92.6	84.1	88.76	11.0	2.5	6.34
MiniCPM-V-2_6, Ovis2-1B, Qwen2.5-VL-72B Step1V, Step1o	95.1	92.6	85.2	88.66	9.9	2.5	6.44
Ovis2-1B, Qwen2.5-VL-72B, Step1V Step1o, bailingMM-Lite	95.1	92.6	85.2	88.66	9.9	2.5	6.44
MiniCPM-V-2_6, Qwen2.5-VL-7B, SenseChat-Vision Step1V, Step1o	95.1	92.6	85.2	88.64	9.9	2.5	6.46
Ovis2-1B, Qwen2.5-VL-7B, Step1V Step1o, bailingMM-Lite	95.1	92.6	85.2	88.56	9.9	2.5	6.54
Qwen-VL-Plus-0809, Qwen2.5-VL-7B, SenseChat-Vision Step1V, Step1o	95.1	92.6	84.3	88.46	10.8	2.5	6.64
GLM4V_PLUS, Ovis2-1B, Qwen2.5-VL-7B Step1V, Step1o	95.1	92.6	84.3	88.38	10.8	2.5	6.72
MUG-U-7B, Qwen-VL-Plus-0809, Step1V							

continued on next page

continuation sheet 12:OCRBench Ensemble Results (5 models)

Models	Score	Max	Min	Avg	Δ_{max}	Δ_{min}	Δ_{avg}
Step1o, bailingMM-Lite	95.1	92.6	84.3	88.36	10.8	2.5	6.74
GLM4V_PLUS, Ovis2-4B, Qwen-VL-Plus-0809 SenseChat-Vision, Step1o	95.1	92.6	84.3	88.30	10.8	2.5	6.80
GLM4V_PLUS, SenseChat-Vision, Step1V Step1o, bailingMM-Lite	95.1	92.6	84.3	88.02	10.8	2.5	7.08
GLM4V_PLUS, Qwen2-VL-72B-Instruct, Step1V Step1o, bailingMM-Lite	95.1	92.6	84.3	87.90	10.8	2.5	7.20
MUG-U-7B, Qwen2.5-VL-72B, SenseChat-Vision Step1V, Step1o	95.0	92.6	87.9	89.92	7.1	2.4	5.08
MUG-U-7B, Ovis2-8B, Qwen2.5-VL-72B Step1V, Step1o	95.0	92.6	87.9	89.90	7.1	2.4	5.10
Ovis2-4B, Qwen2-VL-72B-Instruct, Qwen2.5-VL-72B Step1V, Step1o	95.0	92.6	87.9	89.76	7.1	2.4	5.24
MUG-U-7B, Ovis2-1B, Qwen2.5-VL-7B Step1V, Step1o	95.0	92.6	87.4	89.74	7.6	2.4	5.26
MUG-U-7B, Ovis2-4B, Step1V Step1o, bailingMM-Lite	95.0	92.6	85.2	89.68	9.8	2.4	5.32
InternVL2_5-38B, MUG-U-7B, Ovis2-4B Step1V, Step1o	95.0	92.6	84.1	89.46	10.9	2.4	5.54
MUG-U-7B, Ovis2-1B, Step1V Step1o, bailingMM-Lite	95.0	92.6	85.2	89.30	9.8	2.4	5.70
Ovis2-34B, Ovis2-4B, Qwen2.5-VL-72B SenseChat-Vision, Step1V	95.0	90.9	87.9	89.30	7.1	4.1	5.70
MUG-U-7B, Qwen2-VL-72B-Instruct, Step1V Step1o, bailingMM-Lite	95.0	92.6	85.2	89.26	9.8	2.4	5.74
InternVL2_5-78B-MPO, Ovis2-1B, Qwen2-VL-7B-Instruct SenseChat-Vision, Step1o	95.0	92.6	84.3	89.24	10.7	2.4	5.76
Ovis2-4B, Qwen2.5-VL-72B, SenseChat-Vision Step1o, bailingMM-Lite	95.0	92.6	85.2	89.20	9.8	2.4	5.80
MUG-U-7B, Ovis2-8B, Qwen2-VL-7B-Instruct Step1V, Step1o	95.0	92.6	84.3	89.18	10.7	2.4	5.82
InternVL2_5-78B-MPO, Qwen-VL-Plus-0809, SenseChat-Vision Step1V, Step1o	95.0	92.6	84.3	89.16	10.7	2.4	5.84
Ovis2-4B, Qwen2.5-VL-72B, Step1V Step1o, bailingMM-Lite	95.0	92.6	85.2	89.04	9.8	2.4	5.96
InternVL2_5-38B, MUG-U-7B, Qwen2-VL-72B-Instruct Step1V, Step1o	95.0	92.6	84.1	89.04	10.9	2.4	5.96
MUG-U-7B, NVLM, Qwen2.5-VL-72B Step1V, Step1o	95.0	92.6	84.9	89.02	10.1	2.4	5.98
MiniCPM-V-2_6, Ovis2-1B, Qwen2.5-VL-72B SenseChat-Vision, Step1o	95.0	92.6	85.2	88.82	9.8	2.4	6.18
InternVL2_5-78B, Qwen2.5-VL-7B, SenseChat-Vision Step1V, Step1o	95.0	92.6	85.3	88.66	9.7	2.4	6.34
Ovis2-8B, Qwen2-VL-7B-Instruct, Qwen2.5-VL-72B							

continued on next page

continuation sheet 12:OCRBench Ensemble Results (5 models)

Models	Score	Max	Min	Avg	Δ_{max}	Δ_{min}	Δ_{avg}
Step1V, Step1o	95.0	92.6	84.3	88.54	10.7	2.4	6.46
InternVL2_5-78B, Ovis2-4B, Qwen-VL-Plus-0809 SenseChat-Vision, Step1o	95.0	92.6	84.3	88.50	10.7	2.4	6.50
InternVL2_5-38B, Ovis2-1B, Qwen2.5-VL-7B SenseChat-Vision, Step1o	95.0	92.6	84.1	88.50	10.9	2.4	6.50
Ovis2-4B, Qwen-VL-Plus-0809, Step1V Step1o, bailingMM-Lite	95.0	92.6	84.3	88.32	10.7	2.4	6.68
GLM4V_PLUS, MUG-U-7B, Qwen2-VL-7B-Instruct Step1V, Step1o	95.0	92.6	84.3	88.18	10.7	2.4	6.82
MiniCPM-V-2_6, Ovis2-1B, Qwen2-VL-7B-Instruct SenseChat-Vision, Step1o	95.0	92.6	84.3	88.10	10.7	2.4	6.90
MiniCPM-V-2_6, Qwen-VL-Plus-0809, SenseChat-Vision Step1V, Step1o	95.0	92.6	84.3	88.02	10.7	2.4	6.98
MiniCPM-V-2_6, Ovis2-1B, Qwen-VL-Plus-0809 Step1V, Step1o	95.0	92.6	84.3	87.94	10.7	2.4	7.06
Ovis2-1B, Qwen-VL-Plus-0809, Step1V Step1o, bailingMM-Lite	95.0	92.6	84.3	87.94	10.7	2.4	7.06
GLM4V_PLUS, Qwen-VL-Plus-0809, SenseChat-Vision Step1V, Step1o	95.0	92.6	84.3	87.84	10.7	2.4	7.16

Table 13: OCRBench Ensemble Results (4 models)

Models	Score	Max	Min	Avg	Δ_{max}	Δ_{min}	Δ_{avg}
Ovis2-1B, Qwen2.5-VL-7B, Step1V Step1o	95.5	92.6	87.4	89.40	8.1	2.9	6.10
Qwen2.5-VL-72B, SenseChat-Vision, Step1V Step1o	95.4	92.6	87.9	89.62	7.5	2.8	5.78
MUG-U-7B, Qwen2.5-VL-72B, Step1V Step1o	95.3	92.6	87.9	90.05	7.4	2.7	5.25
MUG-U-7B, Qwen-VL-Plus-0809, Step1V Step1o	95.1	92.6	84.3	89.15	10.8	2.5	5.95
Ovis2-1B, Qwen-VL-Plus-0809, Step1V Step1o	95.1	92.6	84.3	88.62	10.8	2.5	6.47
Ovis2-1B, Qwen2-VL-72B-Instruct, SenseChat-Vision Step1o	95.0	92.6	88.8	89.95	6.2	2.4	5.05
Ovis2-1B, Qwen2.5-VL-72B, Step1V Step1o	95.0	92.6	87.9	89.53	7.1	2.4	5.47
Ovis2-1B, Qwen2-VL-7B-Instruct, SenseChat-Vision Step1o	95.0	92.6	84.3	88.83	10.7	2.4	6.17
MUG-U-7B, Qwen2.5-VL-7B, Step1V Step1o	94.9	92.6	87.4	89.92	7.5	2.3	4.97
Ovis2-1B, SenseChat-Vision, Step1V							

continued on next page

continuation sheet 13: OCRBench Ensemble Results (4 models)

Models	Score	Max	Min	Avg	Δ_{max}	Δ_{min}	Δ_{avg}
Step1o	94.9	92.6	88.6	89.90	6.3	2.3	5.00
Ovis2-1B, Qwen2.5-VL-72B, SenseChat-Vision Step1o	94.9	92.6	87.9	89.72	7.0	2.3	5.17
Qwen2.5-VL-7B, SenseChat-Vision, Step1V Step1o	94.9	92.6	87.4	89.50	7.5	2.3	5.40
SenseChat-Vision, Step1V, Step1o bailingMM-Lite	94.9	92.6	85.2	88.95	9.7	2.3	5.95
Ovis2-1B, Qwen2-VL-7B-Instruct, Step1V Step1o	94.9	92.6	84.3	88.62	10.6	2.3	6.28
MUG-U-7B, Ovis2-4B, Step1V Step1o	94.8	92.6	88.6	90.80	6.2	2.2	4.00
MUG-U-7B, Qwen2-VL-72B-Instruct, Step1V Step1o	94.8	92.6	88.6	90.28	6.2	2.2	4.53
Ovis2-4B, Qwen2.5-VL-7B, Step1V Step1o	94.8	92.6	87.4	89.88	7.4	2.2	4.92
Ovis2-1B, Qwen-VL-Max-0809, SenseChat-Vision Step1o	94.8	92.6	88.1	89.78	6.7	2.2	5.03
MUG-U-7B, SenseChat-Vision, Step1o bailingMM-Lite	94.8	92.6	85.2	89.58	9.6	2.2	5.22
Ovis2-4B, Qwen-VL-Plus-0809, SenseChat-Vision Step1o	94.8	92.6	84.3	89.30	10.5	2.2	5.50
MUG-U-7B, Qwen2-VL-7B-Instruct, Step1V Step1o	94.8	92.6	84.3	89.15	10.5	2.2	5.65
Qwen2-VL-72B-Instruct, SenseChat-Vision, Step1o bailingMM-Lite	94.8	92.6	85.2	89.00	9.6	2.2	5.80
MUG-U-7B, Ovis2-8B, Step1V Step1o	94.7	92.6	88.6	90.40	6.1	2.1	4.30
MUG-U-7B, Qwen2.5-VL-72B, SenseChat-Vision Step1o	94.7	92.6	87.9	90.25	6.8	2.1	4.45
Qwen2-VL-72B-Instruct, SenseChat-Vision, Step1V Step1o	94.7	92.6	88.6	89.85	6.1	2.1	4.85
MUG-U-7B, Qwen2.5-VL-72B, SenseChat-Vision Step1V	94.7	91.1	87.9	89.25	6.8	3.6	5.45
InternVL2_5-26B, Qwen2-VL-72B-Instruct, Step1V Step1o	94.7	92.6	85.4	88.85	9.3	2.1	5.85
Ovis2-1B, Qwen-VL-Plus-0809, SenseChat-Vision Step1o	94.7	92.6	84.3	88.83	10.4	2.1	5.88
Ovis2-1B, Qwen2.5-VL-72B, SenseChat-Vision Step1V	94.7	89.4	87.9	88.72	6.8	5.3	5.97
Qwen2-VL-7B-Instruct, SenseChat-Vision, Step1o bailingMM-Lite	94.7	92.6	84.3	87.88	10.4	2.1	6.83
MUG-U-7B, Ovis2-1B, Step1V Step1o	94.6	92.6	88.6	90.33	6.0	2.0	4.28
MUG-U-7B, Ovis2-1B, Qwen2.5-VL-72B							

continued on next page

continuation sheet 13: OCRBench Ensemble Results (4 models)

Models	Score	Max	Min	Avg	Δ_{max}	Δ_{min}	Δ_{avg}
Step1o	94.6	92.6	87.9	90.15	6.7	2.0	4.45
MUG-U-7B, Qwen2.5-VL-7B, SenseChat-Vision Step1o	94.6	92.6	87.4	90.12	7.2	2.0	4.47
Ovis2-4B, Qwen2.5-VL-72B, Step1V Step1o	94.6	92.6	87.9	90.00	6.7	2.0	4.60
Ovis2-1B, Qwen2-VL-72B-Instruct, Step1V Step1o	94.6	92.6	88.6	89.75	6.0	2.0	4.85
Qwen-VL-Max-0809, SenseChat-Vision, Step1V Step1o	94.6	92.6	88.1	89.67	6.5	2.0	4.92
Ovis2-1B, Qwen2.5-VL-7B, SenseChat-Vision Step1o	94.6	92.6	87.4	89.60	7.2	2.0	5.00
Ovis2-8B, Qwen2.5-VL-7B, Step1V Step1o	94.6	92.6	87.4	89.47	7.2	2.0	5.12
Ovis2-4B, Qwen-VL-Plus-0809, Step1V Step1o	94.6	92.6	84.3	89.10	10.3	2.0	5.50
Qwen-VL-Max-0809, SenseChat-Vision, Step1o bailingMM-Lite	94.6	92.6	85.2	88.83	9.4	2.0	5.78
Qwen2-VL-72B-Instruct, Step1V, Step1o bailingMM-Lite	94.6	92.6	85.2	88.80	9.4	2.0	5.80
Qwen-VL-Plus-0809, SenseChat-Vision, Step1V Step1o	94.6	92.6	84.3	88.72	10.3	2.0	5.88
MUG-U-7B, Ovis2-4B, Qwen2.5-VL-72B Step1o	94.5	92.6	87.9	90.62	6.6	1.9	3.88
MUG-U-7B, Qwen-VL-Max-0809, Step1V Step1o	94.5	92.6	88.1	90.10	6.4	1.9	4.40
Ovis2-34B, Qwen2.5-VL-7B, Step1V Step1o	94.5	92.6	87.4	89.58	7.1	1.9	4.92
MUG-U-7B, Qwen2.5-VL-72B, Step1o bailingMM-Lite	94.5	92.6	85.2	89.20	9.3	1.9	5.30
Ovis2-4B, Qwen2.5-VL-72B, SenseChat-Vision Step1V	94.5	90.9	87.9	89.20	6.6	3.6	5.30
InternVL2_5-38B, MUG-U-7B, Step1V Step1o	94.5	92.6	84.1	89.10	10.4	1.9	5.40
Qwen2.5-VL-72B, SenseChat-Vision, Step1o bailingMM-Lite	94.5	92.6	85.2	88.78	9.3	1.9	5.72
Qwen2-VL-7B-Instruct, SenseChat-Vision, Step1V Step1o	94.5	92.6	84.3	88.72	10.2	1.9	5.78
GLM4V_PLUS, Ovis2-1B, Step1V Step1o	94.5	92.6	84.3	88.62	10.2	1.9	5.88
Ovis2-1B, Qwen2.5-VL-7B, SenseChat-Vision Step1V	94.5	89.4	87.4	88.60	7.1	5.1	5.90
InternVL2_5-38B, Ovis2-1B, Step1V Step1o	94.5	92.6	84.1	88.58	10.4	1.9	5.92
InternVL2_5-38B, Qwen2.5-VL-7B, Step1V							

continued on next page

continuation sheet 13: OCRBench Ensemble Results (4 models)

Models	Score	Max	Min	Avg	Δ_{max}	Δ_{min}	Δ_{avg}
Step1o	94.5	92.6	84.1	88.17	10.4	1.9	6.33
Ovis2-1B, Qwen-VL-Plus-0809, SenseChat-Vision Step1V	94.5	89.4	84.3	87.83	10.2	5.1	6.67
InternVL2_5-78B-MPO, Ovis2-8B, SenseChat-Vision Step1o	94.4	92.6	89.3	90.55	5.1	1.8	3.85
MUG-U-7B, Qwen2-VL-72B-Instruct, SenseChat-Vision Step1o	94.4	92.6	88.8	90.47	5.6	1.8	3.92
Ovis2-4B, Qwen2-VL-72B-Instruct, SenseChat-Vision Step1o	94.4	92.6	88.8	90.42	5.6	1.8	3.98
MUG-U-7B, Ovis2-1B, Qwen2.5-VL-7B Step1o	94.4	92.6	87.4	90.03	7.0	1.8	4.38
MUG-U-7B, Ovis2-4B, Qwen2-VL-72B-Instruct Qwen2.5-VL-72B	94.4	91.1	87.9	89.67	6.5	3.3	4.72
MUG-U-7B, Ovis2-4B, Qwen2.5-VL-72B Step1V	94.4	91.1	87.9	89.62	6.5	3.3	4.78
Ovis2-1B, Qwen-VL-Max-0809, Step1V Step1o	94.4	92.6	88.1	89.58	6.3	1.8	4.83
MUG-U-7B, Ovis2-1B, Qwen2-VL-72B-Instruct Step1V	94.4	91.1	88.6	89.38	5.8	3.3	5.03
MUG-U-7B, Qwen-VL-Plus-0809, SenseChat-Vision Step1o	94.4	92.6	84.3	89.35	10.1	1.8	5.05
MUG-U-7B, Qwen2-VL-7B-Instruct, SenseChat-Vision Step1o	94.4	92.6	84.3	89.35	10.1	1.8	5.05
Ovis2-4B, Qwen2-VL-7B-Instruct, SenseChat-Vision Step1o	94.4	92.6	84.3	89.30	10.1	1.8	5.10
MiniCPM-V-2_6, Ovis2-8B, SenseChat-Vision Step1o	94.4	92.6	85.2	89.12	9.2	1.8	5.28
Qwen-VL-Max-0809, Step1V, Step1o bailingMM-Lite	94.4	92.6	85.2	88.62	9.2	1.8	5.78
InternVL2-76B, Ovis2-1B, Step1V Step1o	94.4	92.6	84.2	88.60	10.2	1.8	5.80
MiniCPM-V-2_6, Qwen2.5-VL-7B, Step1V Step1o	94.4	92.6	85.2	88.45	9.2	1.8	5.95
Qwen2.5-VL-7B, Step1V, Step1o bailingMM-Lite	94.4	92.6	85.2	88.45	9.2	1.8	5.95
GLM4V_PLUS, Qwen2.5-VL-7B, Step1V Step1o	94.4	92.6	84.3	88.22	10.1	1.8	6.17
InternVL2_5-78B-MPO, Ovis2-4B, Step1V Step1o	94.3	92.6	88.6	90.75	5.7	1.7	3.55
Ovis2-4B, Qwen-VL-Max-0809, SenseChat-Vision Step1o	94.3	92.6	88.1	90.25	6.2	1.7	4.05
MUG-U-7B, Ovis2-4B, Step1o bailingMM-Lite	94.3	92.6	85.2	89.95	9.1	1.7	4.35
InternVL2_5-78B-MPO, Qwen2.5-VL-7B, Step1V							

continued on next page

continuation sheet 13: OCRBench Ensemble Results (4 models)

Models	Score	Max	Min	Avg	Δ_{max}	Δ_{min}	Δ_{avg}
Step1o	94.3	92.6	87.4	89.88	6.9	1.7	4.42
Ovis2-8B, Qwen2.5-VL-72B, Step1V Step1o	94.3	92.6	87.9	89.60	6.4	1.7	4.70
Ovis2-4B, Qwen2-VL-72B-Instruct, Step1o bailingMM-Lite	94.3	92.6	85.2	89.38	9.1	1.7	4.92
MiniCPM-V-2_6, Ovis2-4B, Step1V Step1o	94.3	92.6	85.2	89.33	9.1	1.7	4.97
MUG-U-7B, Ovis1.6-Gemma2-27B, Qwen2.5-VL-72B Step1o	94.3	92.6	85.6	89.30	8.7	1.7	5.00
Ovis2-4B, Qwen2.5-VL-72B, Step1o bailingMM-Lite	94.3	92.6	85.2	89.15	9.1	1.7	5.15
MUG-U-7B, Qwen2.5-VL-7B, SenseChat-Vision Step1V	94.3	91.1	87.4	89.12	6.9	3.2	5.17
MUG-U-7B, Qwen2.5-VL-7B, Step1o bailingMM-Lite	94.3	92.6	85.2	89.08	9.1	1.7	5.22
Ovis2-1B, Qwen2-VL-72B-Instruct, Step1o bailingMM-Lite	94.3	92.6	85.2	88.90	9.1	1.7	5.40
Ovis2-1B, Step1V, Step1o bailingMM-Lite	94.3	92.6	85.2	88.85	9.1	1.7	5.45
GLM4V_PLUS, SenseChat-Vision, Step1V Step1o	94.3	92.6	84.3	88.72	10.0	1.7	5.58
InternVL2_5-26B, Qwen-VL-Max-0809, Step1V Step1o	94.3	92.6	85.4	88.67	8.9	1.7	5.62
InternVL2_5-26B, Qwen2.5-VL-72B, Step1V Step1o	94.3	92.6	85.4	88.62	8.9	1.7	5.67
Qwen2.5-VL-72B, Step1V, Step1o bailingMM-Lite	94.3	92.6	85.2	88.58	9.1	1.7	5.72
GLM4V_PLUS, Qwen2-VL-72B-Instruct, Step1V Step1o	94.3	92.6	84.3	88.58	10.0	1.7	5.72
Ovis2-1B, Qwen2.5-VL-7B, Step1o bailingMM-Lite	94.3	92.6	85.2	88.55	9.1	1.7	5.75
MUG-U-7B, Ovis2-4B, Qwen2.5-VL-7B Step1o	94.2	92.6	87.4	90.50	6.8	1.6	3.70
InternVL2_5-78B-MPO, Qwen2-VL-72B-Instruct, SenseChat-Vision Step1o	94.2	92.6	88.8	90.42	5.4	1.6	3.77
Ovis2-4B, Ovis2-8B, Step1V Step1o	94.2	92.6	88.6	90.35	5.6	1.6	3.85
InternVL2_5-78B-MPO, Qwen2-VL-72B-Instruct, Step1V Step1o	94.2	92.6	88.6	90.22	5.6	1.6	3.98
Ovis2-4B, Qwen2-VL-72B-Instruct, Step1V Step1o	94.2	92.6	88.6	90.22	5.6	1.6	3.98
Ovis2-4B, Qwen2.5-VL-72B, SenseChat-Vision Step1o	94.2	92.6	87.9	90.20	6.3	1.6	4.00
InternVL2_5-78B-MPO, MiniCPM-V-2_6, Ovis2-4B							

continued on next page

continuation sheet 13: OCRBench Ensemble Results (4 models)

Models	Score	Max	Min	Avg	Δ_{max}	Δ_{min}	Δ_{avg}
Step1o	94.2	92.6	85.2	89.90	9.0	1.6	4.30
InternVL2_5-78B-MPO, MUG-U-7B, Qwen-VL-Plus-0809							
Step1o	94.2	92.6	84.3	89.72	9.9	1.6	4.47
InternVL2_5-78B-MPO, Ovis2-4B, Qwen2-VL-7B-Instruct							
Step1o	94.2	92.6	84.3	89.67	9.9	1.6	4.53

Table 14: OCRBench Ensemble Results (3 models)

Models	Score	Max	Min	Avg	Δ_{max}	Δ_{min}	Δ_{avg}
Ovis2-8B, SenseChat-Vision, Step1o	94.1	92.6	89.3	90.43	4.8	1.5	3.67
Qwen2.5-VL-7B, Step1V, Step1o	94.0	92.6	87.4	89.53	6.6	1.4	4.47
Ovis2-1B, Step1V, Step1o	94.0	92.6	88.6	90.07	5.4	1.4	3.93
Qwen2-VL-72B-Instruct, Step1V, Step1o	94.0	92.6	88.6	90.00	5.4	1.4	4.00
Ovis2-4B, Qwen2-VL-72B-Instruct, Step1o	94.0	92.6	88.8	90.77	5.2	1.4	3.23
MUG-U-7B, Step1V, Step1o	93.9	92.6	88.6	90.77	5.3	1.3	3.13
MUG-U-7B, Ovis2-4B, Step1o	93.9	92.6	90.9	91.53	3.0	1.3	2.37
MUG-U-7B, Qwen-VL-Plus-0809, Step1o	93.8	92.6	84.3	89.33	9.5	1.2	4.47
Ovis2-4B, Qwen2.5-VL-7B, Step1o	93.8	92.6	87.4	90.30	6.4	1.2	3.50
SenseChat-Vision, Step1V, Step1o	93.8	92.6	88.6	90.20	5.2	1.2	3.60
Ovis2-4B, Qwen-VL-Plus-0809, Step1o	93.7	92.6	84.3	89.27	9.4	1.1	4.43
Ovis2-4B, Step1V, Step1o	93.7	92.6	88.6	90.70	5.1	1.1	3.00
Qwen2-VL-72B-Instruct, SenseChat-Vision, Step1o	93.7	92.6	88.8	90.27	4.9	1.1	3.43
MUG-U-7B, SenseChat-Vision, Step1o	93.7	92.6	89.4	91.03	4.3	1.1	2.67
Ovis2-4B, Qwen2-VL-7B-Instruct, Step1o	93.6	92.6	84.3	89.27	9.3	1.0	4.33
Qwen-VL-Plus-0809, Step1V, Step1o	93.6	92.6	84.3	88.50	9.3	1.0	5.10
Ovis2-4B, Step1o, bailingMM-Lite	93.6	92.6	85.2	89.57	8.4	1.0	4.03
SenseChat-Vision, Step1o, bailingMM-Lite	93.6	92.6	85.2	89.07	8.4	1.0	4.53
Qwen2-VL-72B-Instruct, Step1o, bailingMM-Lite	93.6	92.6	85.2	88.87	8.4	1.0	4.73
MUG-U-7B, SenseChat-Vision, bailingMM-Lite	93.6	91.1	85.2	88.57	8.4	2.5	5.03
MUG-U-7B, Ovis2-4B, Qwen2.5-VL-72B	93.6	91.1	87.9	89.97	5.7	2.5	3.63
Ovis2-4B, Qwen-VL-Max-0809, Step1o	93.6	92.6	88.1	90.53	5.5	1.0	3.07
Qwen-VL-Max-0809, Step1V, Step1o	93.6	92.6	88.1	89.77	5.5	1.0	3.83
Ovis2-8B, Step1V, Step1o	93.6	92.6	88.6	90.17	5.0	1.0	3.43
Ovis2-4B, SenseChat-Vision, Step1o	93.6	92.6	89.4	90.97	4.2	1.0	2.63
Qwen-VL-Plus-0809, SenseChat-Vision, Step1o	93.5	92.6	84.3	88.77	9.2	0.9	4.73
Qwen2-VL-7B-Instruct, Step1V, Step1o	93.5	92.6	84.3	88.50	9.2	0.9	5.00
MUG-U-7B, Ovis1.6-Gemma2-27B, Step1o	93.5	92.6	85.6	89.77	7.9	0.9	3.73

continued on next page

continuation sheet 14: OCRBench Ensemble Results (3 models)

Models	Score	Max	Min	Avg	Δ_{max}	Δ_{min}	Δ_{avg}
MUG-U-7B, Qwen2.5-VL-7B, Step1o	93.5	92.6	87.4	90.37	6.1	0.9	3.13
Qwen2.5-VL-72B, SenseChat-Vision, Step1o	93.5	92.6	87.9	89.97	5.6	0.9	3.53
MUG-U-7B, Ovis2-4B, Step1V	93.5	91.1	88.6	90.20	4.9	2.4	3.30
MUG-U-7B, Step1o, bailingMM-Lite	93.4	92.6	85.2	89.63	8.2	0.8	3.77
Ovis2-34B, Step1V, Step1o	93.4	92.6	88.6	90.30	4.8	0.8	3.10
MUG-U-7B, Qwen2-VL-72B-Instruct, Step1V	93.4	91.1	88.6	89.50	4.8	2.3	3.90
MUG-U-7B, Qwen2-VL-72B-Instruct, Step1o	93.4	92.6	88.8	90.83	4.6	0.8	2.57
MUG-U-7B, Qwen2-VL-7B-Instruct, Step1o	93.3	92.6	84.3	89.33	9.0	0.7	3.97
Ovis2-8B, Step1o, bailingMM-Lite	93.3	92.6	85.2	89.03	8.1	0.7	4.27
Step1V, Step1o, bailingMM-Lite	93.3	92.6	85.2	88.80	8.1	0.7	4.50
Qwen2.5-VL-72B, Step1o, bailingMM-Lite	93.3	92.6	85.2	88.57	8.1	0.7	4.73
Ovis2-8B, Qwen2.5-VL-7B, Step1o	93.3	92.6	87.4	89.77	5.9	0.7	3.53
MUG-U-7B, Qwen2.5-VL-7B, Step1V	93.3	91.1	87.4	89.03	5.9	2.2	4.27
Ovis2-4B, Qwen2.5-VL-72B, Step1o	93.3	92.6	87.9	90.47	5.4	0.7	2.83
Ovis2-8B, Qwen2-VL-72B-Instruct, Step1o	93.3	92.6	88.8	90.23	4.5	0.7	3.07
Ovis2-1B, SenseChat-Vision, Step1o	93.3	92.6	89.0	90.33	4.3	0.7	2.97
Ovis2-34B, SenseChat-Vision, Step1o	93.3	92.6	89.4	90.57	3.9	0.7	2.73
InternVL2_5-38B, Step1V, Step1o	93.2	92.6	84.1	88.43	9.1	0.6	4.77
NVLM, Ovis2-4B, Step1o	93.2	92.6	84.9	89.47	8.3	0.6	3.73
Qwen2.5-VL-7B, SenseChat-Vision, Step1o	93.2	92.6	87.4	89.80	5.8	0.6	3.40
Qwen2.5-VL-72B, Step1V, Step1o	93.2	92.6	87.9	89.70	5.3	0.6	3.50
Qwen-VL-Max-0809, SenseChat-Vision, Step1o	93.2	92.6	88.1	90.03	5.1	0.6	3.17
MUG-U-7B, Ovis2-4B, Qwen2-VL-72B-Instruct	93.2	91.1	88.8	90.27	4.4	2.1	2.93
Ovis2-1B, Qwen2-VL-72B-Instruct, Step1o	93.2	92.6	88.8	90.13	4.4	0.6	3.07
MUG-U-7B, Ovis2-8B, Step1o	93.2	92.6	89.3	91.00	3.9	0.6	2.20
MUG-U-7B, NVLM, Step1o	93.1	92.6	84.9	89.53	8.2	0.5	3.57
Qwen-VL-Max-0809, Step1o, bailingMM-Lite	93.1	92.6	85.2	88.63	7.9	0.5	4.47
Qwen2.5-VL-7B, Step1o, bailingMM-Lite	93.1	92.6	85.2	88.40	7.9	0.5	4.70
MUG-U-7B, Ovis2-4B, Qwen2.5-VL-7B	93.1	91.1	87.4	89.80	5.7	2.0	3.30
MUG-U-7B, Qwen2.5-VL-72B, Step1o	93.1	92.6	87.9	90.53	5.2	0.5	2.57
MUG-U-7B, Qwen-VL-Max-0809, Step1o	93.1	92.6	88.1	90.60	5.0	0.5	2.50
Ovis2-8B, Qwen-VL-Max-0809, Step1o	93.1	92.6	88.1	90.00	5.0	0.5	3.10
MUG-U-7B, SenseChat-Vision, Step1V	93.1	91.1	88.6	89.70	4.5	2.0	3.40
GLM4V_PLUS, MUG-U-7B, Step1o	93.0	92.6	84.3	89.33	8.7	0.4	3.67
MUG-U-7B, Qwen-VL-Plus-0809, Step1V	93.0	91.1	84.3	88.00	8.7	1.9	5.00
NVLM, Step1V, Step1o	93.0	92.6	84.9	88.70	8.1	0.4	4.30
MUG-U-7B, Ovis2-4B, Qwen-VL-Max-0809	93.0	91.1	88.1	90.03	4.9	1.9	2.97

continued on next page

continuation sheet 14: OCRBench Ensemble Results (3 models)

Models	Score	Max	Min	Avg	Δ_{max}	Δ_{min}	Δ_{avg}
MUG-U-7B, Qwen-VL-Max-0809, Step1V	93.0	91.1	88.1	89.27	4.9	1.9	3.73
MUG-U-7B, Ovis2-34B, Step1o	93.0	92.6	89.7	91.13	3.3	0.4	1.87
InternVL2_5-78B-MPO, MUG-U-7B, Step1o	93.0	92.6	90.9	91.53	2.1	0.4	1.47
Qwen-VL-Plus-0809, Step1o, bailingMM-Lite	92.9	92.6	84.3	87.37	8.6	0.3	5.53
MUG-U-7B, Ovis2-1B, bailingMM-Lite	92.9	91.1	85.2	88.43	7.7	1.8	4.47
InternVL2_5-26B, Ovis2-4B, Step1o	92.9	92.6	85.4	89.63	7.5	0.3	3.27
MUG-U-7B, Qwen2.5-VL-72B, SenseChat-Vision	92.9	91.1	87.9	89.47	5.0	1.8	3.43
MUG-U-7B, Qwen2.5-VL-72B, Step1V	92.9	91.1	87.9	89.20	5.0	1.8	3.70
Ovis2-4B, Qwen2.5-VL-72B, Step1V	92.9	90.9	87.9	89.13	5.0	2.0	3.77
Ovis2-4B, Qwen2-VL-72B-Instruct, Step1V	92.9	90.9	88.6	89.43	4.3	2.0	3.47
Ovis2-4B, Qwen2-VL-72B-Instruct, SenseChat-Vision	92.9	90.9	88.8	89.70	4.1	2.0	3.20
MUG-U-7B, Ovis2-1B, Step1o	92.9	92.6	89.0	90.90	3.9	0.3	2.00
InternVL2-76B, Qwen2-VL-72B-Instruct, Step1o	92.8	92.6	84.2	88.53	8.6	0.2	4.27
Qwen2-VL-7B-Instruct, SenseChat-Vision, Step1o	92.8	92.6	84.3	88.77	8.5	0.2	4.03
MUG-U-7B, Qwen2-VL-7B-Instruct, Step1V	92.8	91.1	84.3	88.00	8.5	1.7	4.80
Qwen2-VL-7B-Instruct, Step1o, bailingMM-Lite	92.8	92.6	84.3	87.37	8.5	0.2	5.43
NVLM, SenseChat-Vision, Step1o	92.8	92.6	84.9	88.97	7.9	0.2	3.83
NVLM, Ovis2-8B, Step1o	92.8	92.6	84.9	88.93	7.9	0.2	3.87
MUG-U-7B, MiniCPM-V-2_6, Step1o	92.8	92.6	85.2	89.63	7.6	0.2	3.17
MUG-U-7B, Step1V, bailingMM-Lite	92.8	91.1	85.2	88.30	7.6	1.7	4.50
Ovis2-4B, Qwen2.5-VL-72B, bailingMM-Lite	92.8	90.9	85.2	88.00	7.6	1.9	4.80
InternVL2_5-78B, Step1V, Step1o	92.8	92.6	85.3	88.83	7.5	0.2	3.97
Ovis2-4B, Qwen2.5-VL-7B, Step1V	92.8	90.9	87.4	88.97	5.4	1.9	3.83
Ovis2-1B, Qwen2.5-VL-7B, Step1V	92.8	89.0	87.4	88.33	5.4	3.8	4.47
Ovis2-8B, Qwen2.5-VL-72B, Step1o	92.8	92.6	87.9	89.93	4.9	0.2	2.87
Ovis2-1B, Qwen2.5-VL-72B, Step1o	92.8	92.6	87.9	89.83	4.9	0.2	2.97
Ovis2-4B, Qwen2.5-VL-72B, SenseChat-Vision	92.8	90.9	87.9	89.40	4.9	1.9	3.40
MUG-U-7B, Ovis2-1B, Ovis2-4B	92.8	91.1	89.0	90.33	3.8	1.7	2.47
Ovis2-1B, Qwen-VL-Plus-0809, Step1o	92.7	92.6	84.3	88.63	8.4	0.1	4.07
Ovis2-1B, Qwen2-VL-7B-Instruct, Step1o	92.7	92.6	84.3	88.63	8.4	0.1	4.07
InternVL2_5-78B, Qwen2-VL-7B-Instruct, Step1o	92.7	92.6	84.3	87.40	8.4	0.1	5.30
NVLM, Qwen2-VL-72B-Instruct, Step1o	92.7	92.6	84.9	88.77	7.8	0.1	3.93
Ovis2-34B, Step1o, bailingMM-Lite	92.7	92.6	85.2	89.17	7.5	0.1	3.53
MUG-U-7B, Qwen2-VL-72B-Instruct, bailingMM-Lite	92.7	91.1	85.2	88.37	7.5	1.6	4.33
Ovis2-4B, Qwen2-VL-72B-Instruct, bailingMM-Lite	92.7	90.9	85.2	88.30	7.5	1.8	4.40

J LIMITATIONS AND FUTURE DIRECTIONS

Despite the promising results demonstrated by the Consensus Entropy framework, several limitations warrant acknowledgment and suggest avenues for future research. The current implementation relies on semantic embedding spaces that may not fully capture the nuances of

specialized domains such as mathematical formulas or chemical notations. Additionally, the framework's performance is contingent on having multiple independent VLMs available at inference time, which may impose computational constraints in resource-limited scenarios. The optimal threshold for routing decisions currently requires empirical calibration for each specific application domain, limiting immediate out-of-the-box deployment.

Future research directions could address these limitations through domain-specific embedding techniques for specialized content types, more efficient ensemble methods requiring fewer models, and adaptive threshold mechanisms that automatically adjust to document characteristics. Additional investigations into the theoretical properties of prediction convergence patterns could lead to more principled frameworks for uncertainty quantification beyond the OCR domain. The insights from these convergence patterns might also inform model design and training objectives, potentially enhancing individual model robustness. Exploring the relationship between model architecture diversity and ensemble effectiveness represents another promising direction, particularly in identifying minimal but complementary model combinations that maximize performance gains while minimizing computational overhead.

OCR Human Evaluation Tool

Reload ./data.jsonl and ./image

Image Preview

OMBRE—OMEN

northwest of Timor, from which the Ombay Pass, in the line of one of the best routes from Europe to China, separates it. It is about 900 square miles in extent, 65 miles long, and 15 broad, and presents a bold coast and lofty interior. The mountains are covered to their summits with lofty trees. It is inhabited by savage tribes, said to be fierce and treacherous, and carries on some trade with Timor in birds' nests and provisions, exchanged for iron-work, Chinese wares and linen, Allor on the northwest and Baloko on the southeast being the chief settlements and ports. It belongs to the Netherlands, and is included in the residency of Timor.

Ombre, óm'bér, a game of cards originating in Spain. It is usually played by three persons, with 40 cards (the eights, nines, and tens having been removed), and each player receives nine cards, three by three. The game is often mentioned in English 18th century literature.

Omdurman, óm-door'mán, Sudan, a native town on the White Nile, opposite Khartum. It was built as the capital of the Mahdi's successor, when Khartum was destroyed in 1885, and extends for four miles along the river bank. Under the Khalifa Abdallah it had a population of 60,000 inhabitants, living in one-storied mud huts, lining streets laid out on an orderly system, and guarded by a walled enclosure flanked with towers, accommodating 10,000 warriors. When the Khalifa was defeated, 2 Sept. 1898, Omdurman was hastily deserted, but with returning trade and prosperity has (1904) an estimated population of 60,000. Omdurman is the great mart of the gum-arabic, ivory, and ostrich-feather trade of northeastern Africa, and representatives of over thirty tribes congregate in its markets.

O'Meara, ó-má'ra, Barry Edward, English physician; b. Ireland 1778; d. London 3 June 1836. He was household physician to the Emperor Napoleon I. at Saint Helena, and published 'Napoleon in Exile' (1822). Originally a surgeon in the British navy, he was serving on the Bellerophon in that capacity 7 Aug. 1815 when Napoleon went on board. Napoleon noting O'Meara's skill and knowledge of Italian, desired the surgeon to accompany him to Saint Helena. Having obtained Admiral Keith's permission, O'Meara remained with the ex-emperor till July 1818. He was then recalled and deprived of his rank, for having accused Sir Hudson Lowe before the admiralty of cruel and arbitrary conduct.

Omega, ó-mé'ga or ó-még'a, the last letter of the Greek alphabet; hence, figuratively speaking, the end or last of anything. See ALPHABET.

Omen, a sign believed to prognosticate a future event, between which and the event foretold there appears no relation of cause and effect, but which is usually received as an intimation from a superior power. Omens have been common among most nations, and are often remembered and mentioned after they have ceased to be credited. Though generally classed among superstitions, they may sometimes be founded on some hidden relation in things, some natural law of sequence the ground of which is unknown. They have been chiefly in vogue in the ruder ages and communities, though under the name of auguries they retained their influence during the whole period of pagan antiquity, and though eminent warriors and other popular leaders in moments of extreme doubt and peril have given notable examples of faith in them. Sneezing was deemed ominous in the time of Homer, and Eustathius states that it was lucky or unlucky according as it was directed to the right or the left. Aristotle discusses the problem why sneezing from noon to midnight is good, and from midnight to noon bad. At noon it was propitious. Among the ancient Persians sneezing was esteemed fortunate, a sign of contest between the fiery soul and the earthly body, and of the victory of the former. When the emperor of Monomotapa sneezes, says Codrigan, it is proclaimed through the whole land as a signal for general joy. The itching of the nose implied that a stranger was coming. Burton, in his 'Anatomy of Melancholy', states that "to bleed three drops at the nose is an ill omen." The spots on the finger nails were all ominous; the itching of the palm of the right hand promised a receipt of money; the doubling of the thumb within the hand was believed to have efficacy in avoiding approaching danger, and therefore the thumbs of dead persons were so folded. The way in which fishes, canes, or lamps burned suggested divers omens. The superstition still prevails in many places that the howling of a dog by night presages a death in the neighborhood. Duncan Campbell expresses his faith in this omen, and adds: "Odd and unaccountable as it may seem, those animals scent death, even before it seizes a person." The screeching of the owl and the croaking of the raven have both in ancient and modern times been regarded as omens of some dire calamity. Divers presages concerning the weather have been derived from the habits of birds, bees, wasps, gnats, etc. Pennant states that many of the great families of Scotland received monitions of future events, especially of death, by spectres, wraiths, and shiricks. Fishermen and sailors discover omens in echoes, flashes, shadows, and other visible appearances. To throw a cat overboard, or lose a bucket, is believed to be unlucky. Whistling is supposed to stir up the wind. Stumbling has been the subject of numerous superstitions. Gaius Gracchus stumbled at his threshold on the morning of his death. To stumble on going out, says Bishop Hall, was mischievous; to stumble up stairs, says Grose, was lucky.

At the present day, in many parts of England and the United States, a superstitious belief in omens exists. It is regarded as unlucky to see first one magpie and then more; but two denote marriage or merriment; three, a successful journey; four, an unexpected piece of good news; five, that you will shortly be in a great company. To kill a magpie is to incur some terrible misfortune. When a person goes out on any important business, it is lucky to throw an old shoe after him. To present a knife, scissors, razor, or other sharp or cutting instrument to one's friend is unlucky, as they are apt to divide love and friendship. The falling of salt toward persons at table, the spilling of wine on their clothes, are evil omens. Breaking a looking glass betokens the death of the best friend of the person to whom it belonged. The burning of the cheeks, or tingling of the ears, that others were talking of us; if of the

OCR Recognition Content (LaTeX/Markdown source)

****OMBRE—OMEN****

...

northwest of Timor, from which the Ombay Pass, in the line of one of the best routes from Europe to China, separates it. It is about 900 square miles in extent, 65 miles long, and 15 broad, and presents a bold coast and lofty interior. The mountains are covered to their summits with lofty trees. It is inhabited by savage tribes, said to be fierce and treacherous, and carries on some trade with Timor in birds' nests and provisions, exchanged for iron-work, Chinese wares and linen, Allor on the northwest and Baloko on the southeast being the chief settlements and ports. It belongs to the Netherlands, and is included in the residency of Timor.

****Ombre****, óm'bér, a game of cards originating in Spain. It is usually played by three persons, with 40 cards (the eights, nines, and tens having been removed), and each player receives nine cards, three by three. The game is often mentioned in English 18th century literature.

****Omdurman****, óm-door'mán, Sudan, a native town on the White Nile, opposite Khartum. It was built as the capital of the Mahdi's successor, when Khartum was destroyed in 1885, and extends for four miles along the river bank. Under the Khalifa Abdallah it had a population of 500,000 inhabitants, living in one-storied mud huts, lining streets laid out on an orderly system, and guarded by a walled enclosure flanked with towers, accommodating 10,000 warriors. When the Khalifa was defeated, 2 Sept. 1898, Omdurman was hastily deserted, but with returning trade and prosperity has (1904) an estimated population of 60,000. Omdurman is the great mart of the gum-arabic, ivory, and ostrich-feather trade of northeastern Africa, and representatives of over thirty tribes congregate in its markets.

Current Status

Index: 24 | 25 / 1000 | Not scored

1 Completely Correct

2 Minor Errors

3 Partially Correct

4 Mostly Incorrect

← Previous

Skip

Next →

Jump to index (not sequence number)

20 Jump

Figure 14: OCR Human Evaluation Interface: This annotation tool enables efficient assessment of OCR quality across multiple models. The interface displays the source image alongside OCR results, allowing annotators to assign quality scores based on a standardized 4-level rating system (from completely correct to mostly incorrect). The tool tracks progress, enables navigation between samples, and supports targeted image selection, facilitating comprehensive human evaluation of OCR performance on real-world data.